Synthesis & Characterization of $LiFe_{1-X}Ni_XPO_4/C$ $(0 \leq X \leq 1)$

Abhinaba Sinha

Synthesis & Characterization of $LiFe_{1-X}Ni_XPO_4/C$ ($0 \leq X \leq 1$)

A report submitted in partial fulfillment of the requirements for the degree of

Master of Technology
In
Nanoscience & Technology

Submitted
By
Abhinaba Sinha
Roll No. – 2K11/NST/01

Under the guidance of

Dr. Amrish Panwar

Department of Applied Physics
Delhi Technological University
Delhi-110042

Candidate's Declaration

I hereby declare that the work which is being presented in this thesis entitled **"Synthesis and Characterization of $LiFe_{1-X}Ni_XPO_4/C$"** is my own work carried out under the guidance of Dr. Amrish Panwar, Assistant Professor, DTU New Delhi. I further declare that the matter embodied in this thesis has not been submitted for the award of any other degree or diploma.

Date: **Abhinaba Sinha**

Place: New Delhi Roll. No. 2k11/NST/01

Department of Applied Physics
Delhi Technological University
Delhi – 110042,
India

CERTIFICATE

This is to certify that this report entitled "**Synthesis & Characterization of $LiFe_{1-x}Ni_xPO_4/C$"** submitted by Abhinaba Sinha to the Department of Applied Physics, Delhi Technological University, Delhi in partial fulfillment of the requirements for the award of the degree of Master of Technology in July 2013 is an authentic record of the work carried out under my guidance and supervision.

In my opinion, this work fulfills the requirement for which it has been submitted. This report has not been submitted to any other university or institution for any degree or diploma.

Dr Amrish Panwar
Assistant Professor
Dept. of Applied Physics
DTU

Prof S C Sharma
Head of the Department
Dept. of Applied Physics
DTU

ACKNOWLEDGEMENT

I would like to express my deepest and utmost gratitude to my supervisor Dr Amrish Panwar without whose encouragement, guidance, patience and support this work would have been incomplete. I would also like to express my gratitude to Dr. S. Ghosh & Dr. S. Aich (Dept. of MME, IIT Kharagpur) for their invaluable guidance in all respect to complete this work.

My sincere thanks to Dr Pawan Kumar Tyagi & Dr Jayasimhadri M, who showed immense kindness by allowing me to use their laboratories.

I humbly extend my words of gratitude to other faculty members and our Head of the Department Prof S Sharma, staff and administration of this department for providing me the valuable support and time whenever required.

I am deeply grateful to the Mr. Vinay Kumar, Ms Lucky Krishnia, Mrs Ritu and Mr Amit Vishwakarma, Mr. Parijat Pallab Jana, Mr. Pranabananda Modak for helping me to prepare samples in Laboratories.

I am also indebted to Mr Uttam,Mr. Ranadeep Basu, Mr. Gautam Sau, Mr Atanu Sau, Mr Basudev Debnath, Mr Premchand and Mr Nitai Pal.

I humbly extend my words of gratitude to my friend Mr. Sandeep Prajapati, Mr. E. Jayakumar, Mr. Pavan Polkampally for helping me to perform this work.

LIST OF TABLES

LIST OF FIGURES

ABSTRACT

The major contribution to the battery performance is due to the cathode material. The present work attributes to finding a novel cathode material which would have high cell voltage, high life cycle, high specific energy, safety and economical.

Ge et al. found that when $LiFePO_4$/C was doped with Nickel, the cycle life was enhanced from nearly 2000 (commercially available Lib) to around 5500-7200. This was a remarkable achievement. The composition of the nickel doped $LiFePO_4$ was not revealed. Moreover $LiNiPO_4$ has been found to have a very high cell voltage of 5.1 Volt. It was strongly felt that for a suitable doping percentage of Nickel in $LiFe_{1-X}Ni_XPO_4$ ($0 \leq X \leq 1$), we can get a composition having very high cell voltage and high life cycle. $LiFePO_4$ & $LiNiPO_4$ were successfully synthesized but $LiFe_{1-X}Ni_XPO_4$ (X= 0.125, 0.250, 0.375) were tried but no phase was formed.

TABLE OF CONTENTS

Chapter 1: Introduction

The fast consumption of the fossil fuels such as petroleum, coal, natural gases etc have compelled the researchers to look for green energy sources such as solar energy, hydroelectric energy, wind energy and electrical energy storage such as Lithium ion battery. Among the alternatives to the non renewable sources of energy, Lithium ion battery is considered to be a most promising option for fossil fuel energy sources because of its high energy density [1].

1.1 History of Battery Development

A battery is a transducer which converts chemical energy into electrical energy and vice versa. The first battery was invented in the year 1798 by Italian physicist Alessandro Volta. After a period of four decades, Daniel Cell was invented. It offered better cell voltage and also eliminated the hydrogen bubble problem in Voltaic Cell. With the passage of time, many important achievements took place in the history of battery development. The first was the invention of rechargeable Lead Acid cell. Until recent past, an improved version of Lead Acid Cell was used as car battery. Gradually, wet electrolyte cells were replaced by dry electrolyte cells. This led to the development of portable batteries. Soon after this, alkaline batteries came into existence [2, 3].

With the rapid advancement in the field of electronic industry and the invention of wide varieties of electronic goods, the need for a high energy to weight ratio and high electrochemical potential material was increasingly felt. The lithium ion batteries offer 2-3 times higher energy density and 5-6 times higher power density than conventional Ni-Cd and Ni-MH batteries. This led to the invention of Lithium ion battery [4]. The first commercial Lithium ion battery was introduced by Sony Corporation, Japan in 1991-92 [4]. Since then researchers are continuously trying to develop improved version of Lithium Ion battery. Because of the reduced size of Lithium ion batteries, it is used in mobile phones, laptops, iPods, iPads, tablet PCs and many more things [3]. Figure 1 shows the charging and discharging process in a lithium ion battery.

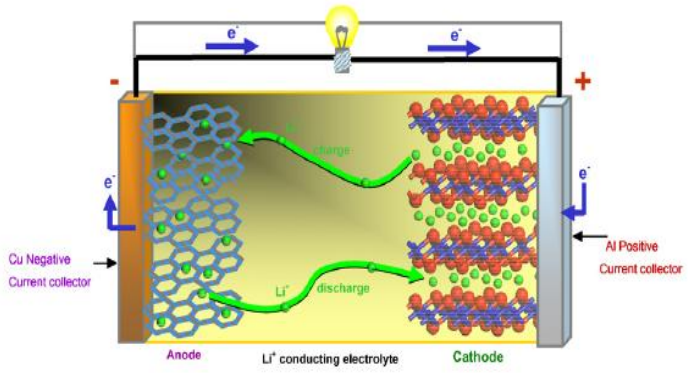

Figure 1: Lithium ion battery (Charging and Discharging) [4]

The development of Lithium ion battery broadly depends on three factors [6]:

1. Cathode, Anode and Electrolyte Materials.

2. Geometry of the battery.

3. Battery Management System.

Out of the three factors, the most important is cathode material as the discharge potential, specific capacity, cycle life etc. depends on the cathode materials [7]. The limitations of the Lithium Ion Battery are its cost and safety [8]. Table 1 summarizes the components, materials and functions of Lithium ion Battery.

Components	Functions	Materials
Cathode	• Emit lithium-ion to anode during charging • Receive lithium-ion during discharging	lithium metal oxide powder
Anode	• Receive lithium-ion from anode during charging • Emit lithium-ion during discharging	Graphite powder
Electrolyte	• Pass lithium-ions between cathode and anode	Lithium salts and organic solvents
Separator	• Prevent short circuit between cathode and anode • Pass lithium ions through pores in separator	Micro-porous membranes

Source: CGGC

Table 1: LIB components and Functions

The present focus of researchers is to develop high energy density, high cycle life, economical, environment friendly and safe cathode material by various means. $LiCoO_2$ was the first cathode

material which was used in lithium ion battery. It is no doubt a good cathode material but has the disadvantage of being costly and toxic due to the presence of cobalt in it. These limitations can be overcome by using $LiFePO_4$ because of its being non toxic, having high discharge potential (around 3.4 V), large specific capacity (170 mAh/g) and inexpensive. $LiFePO_4$ has an olivine structure. Its biggest disadvantage is the low electronic conductivity (10^{-9} Scm^{-1}). A lot of effort has been made to sort out this problem and optimize $LiFePO_4$. This problem can be broadly solved by following ways [4, 5, 10-15]:

1. Coating $LiFePO_4$ with Carbon.
2. Decreasing the size of particles.
3. Doping with other ions.
4. Improving the Micro structural Characteristics.

$LiFePO_4$ can be prepared by various processes. Each process has certain inherent advantages and disadvantages associated with it. All these processes have been thoroughly investigated and have been presented in the next section. Among all other processes, the author found that Sol Gel technique is one of the promising routes for the synthesis of cathode Material [4, 7].

1.2 OBJECTIVE

- To Synthesize $LiFe_{1-x}Ni_xPO_4/C$ ($0 \leq X \leq 1$) in order to find a novel cathode material by economical Sol Gel Route.
- Characterization of $LiFe_{1-x}Ni_xPO_4/C$ ($0 \leq X \leq 1$) using X-Ray Diffractometer Analysis (XRD), Field Emission Scanning Electron Microscopy(FESEM) & High Resolution Transmission electron Microscopy(HRTEM).

Chapter 2: Literature Review

2.1 Lithium Ion Battery (LIB)

Lithium ion batteries have revolutionized our lives. From mobile phones, laptops, cameras, iPods, mp3 players etc., every where it is used. It has become part & parcel of our life.

The history of battery development has been discussed in the last section. In the present section, working principle, components, synthesis, global market trend of Lithium ion Battery and research on optimization of cathode material has been discussed thoroughly. The major use of Lithium ion battery is in defense sector. All superpower countries are trying to indigenously develop lithium ion Battery manufacturing units in their own countries. Figure 2 shows the global market share of different countries in Lithium ion Battery Industry.

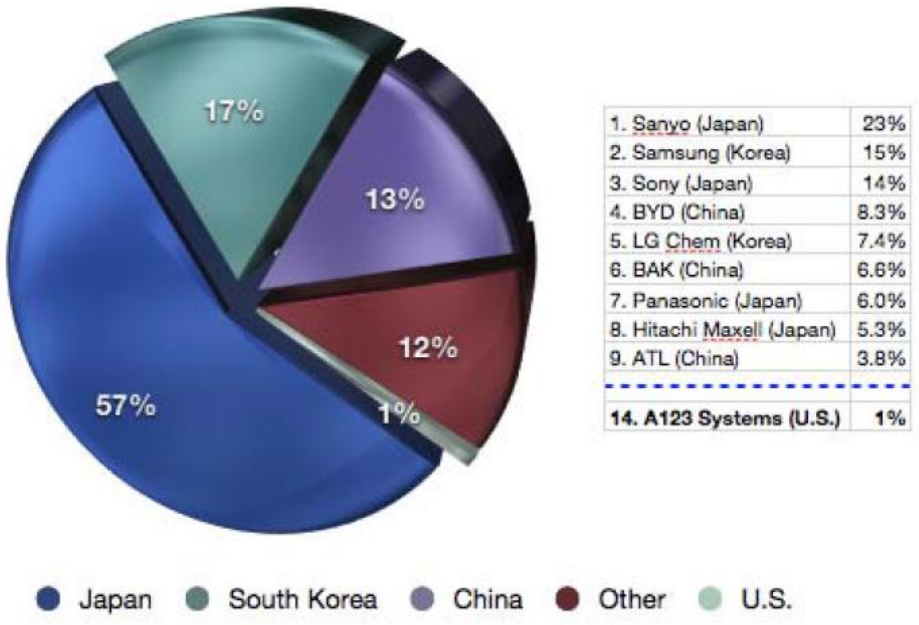

1. Sanyo (Japan)	23%
2. Samsung (Korea)	15%
3. Sony (Japan)	14%
4. BYD (China)	8.3%
5. LG Chem (Korea)	7.4%
6. BAK (China)	6.6%
7. Panasonic (Japan)	6.0%
8. Hitachi Maxell (Japan)	5.3%
9. ATL (China)	3.8%
14. A123 Systems (U.S.)	**1%**

Source: CGGC, based on(METI, 2010; NEDO, 2009)

Figure 2: Global Market Share of Lithium ion Battery Industry

The price of Lithium ion batteries have been projected to come at par with Ni-MH and Lead Acid Cell by 2020. This has been shown in the Figure 3.

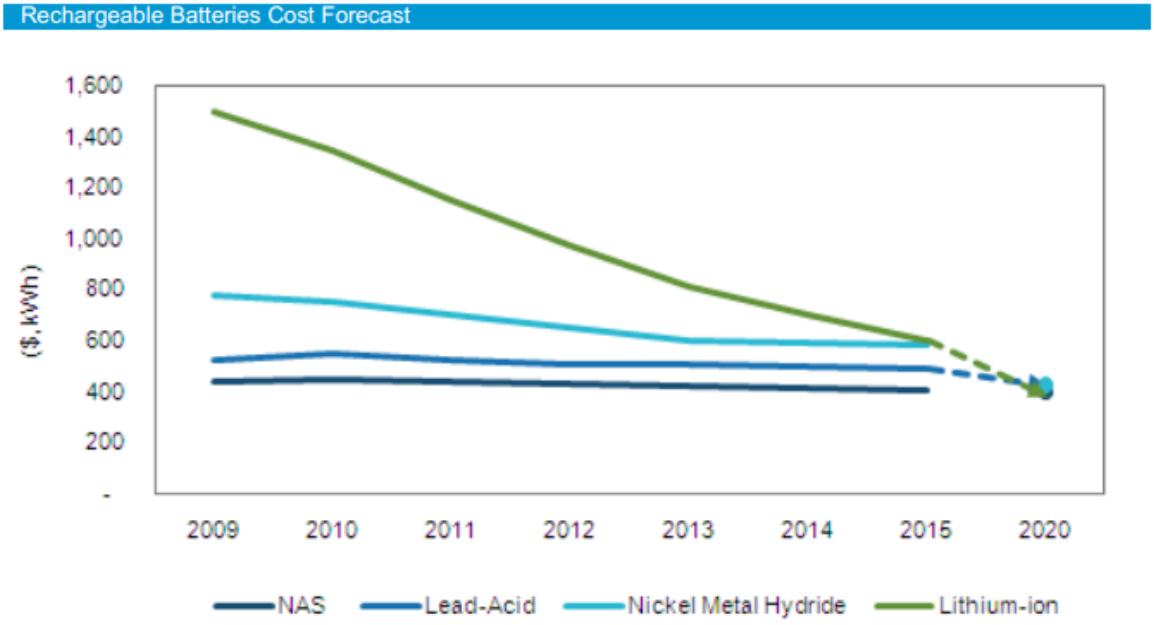

Figure 3: Lithium ion battery cost projection [41]

Lithium ion battery is going to play a big role in the nearby future. Figure 4 shows the US investment in LIB sector in the coming years. It shows an increasing trend which means LIB market is going to rise.

Figure 4: US investment in Lithium ion battery industry [42]

2.2 Comparison between LIB and other batteries

A Comparative study between the properties of different kinds of secondary cells is given below to show the superiority of Lithium ion Battery over other batteries [16].

Specifications	Lead Acid	NiCd	NiMH	Li-ion		
				Cobalt	Manganese	Phosphate
Specific energy density (Wh/kg)	30–50	45–80	60–120	150–190	100–135	90–120
Internal resistance[1] (mΩ)	<100 12V pack	100–200 6V pack	200–300 6V pack	150–300 7.2V	25–75[2] per cell	25–50[2] per cell
Cycle life[4] (80% discharge)	200–300	1000[3]	300–500[3]	500–1,000	500–1,000	1,000–2,000
Fast-charge time	8–16h	1h typical	2–4h	2–4h	1h or less	1h or less
Overcharge tolerance	High	Moderate	Low	Low. Cannot tolerate trickle charge		
Self-discharge/ month (room temp)	5%	20%[5]	30%[5]	<10%[6]		
Cell voltage (nominal)	2V	1.2V[7]	1.2V[7]	3.6V[8]	3.8V[8]	3.3V
Charge cutoff voltage (V/cell)	2.40 Float 2.25	Full charge detection by voltage signature		4.20		3.60
Discharge cutoff voltage (V/cell, 1C)	1.75	1.00		2.50 – 3.00		2.80
Peak load current Best result	5C[9] 0.2C	20C 1C	5C 0.5C	>3C <1C	>30C <10C	>30C <10C
Charge temperature	–20 to 50°C	0 to 45°C		0 to 45°C[10]		
Discharge temperature	–20 to 50°C	–20 to 65°C		–20 to 60°C		
Maintenance requirement	3–6 months[11] (topping chg.)	30–60 days (discharge)	60–90 days (discharge)	Not required		
Safety requirements	Thermally stable	Thermally stable, fuse protection common		Protection circuit mandatory[12]		
In use since	Late 1800s	1950	1990	1991	1996	1999

Table 2: Comparative Study of the properties of different batteries [16]

From the above comparison it can be seen that Lithium Ion Battery has edge over other contemporary batteries. Lithium ion batteries have the following advantages:

i. High Specific Energy.
ii. High cycle Life.
iii. Less charging Time.
iv. High Cell Voltage.
v. Maintenance free.

The only issue with LIB is its safety. A considerable amount of research effort has been invested in developing safer LIB, and development of more effective thermal management system and protection devices. Very often lithium ion batteries have been found to be explosive. There are many causes behind this [17]:

i. Thermal runaway of Lithium ion batteries.
ii. Electrolyte decomposition and evolution of gas from lib.

2.3 LIB Components

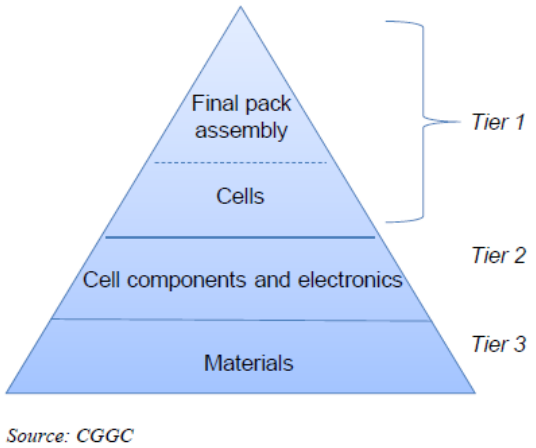

Figure 5: Different Tiers of Lithium ion Battery

There are three main internal components of a L-ion Battery :

1. Cathode Material:
2. Anode Material:
3. Electrolyte:

There are three main external components of Lithium ion Battery :

1. Battery Cell
2. Battery Module
3. Battery Pack

Source:(Hitachi Vehicle Energy, 2008; Magna, 2010)

Figure 6: LIB External Components

2.3.1 Cathode Material

A battery system has many terminologies. These are:

- C- Rate: Discharge rate is denoted by the C rate. 1 C means that the cell will lose its charge in 1hr. Similarly a discharge rate of 2C means that the cell will lose its charge in 30 minutes.

- Cycle Life: The number of charge-discharge cycles which a cell can undergo before its performance goes down.

- Specific Energy: The battery energy per unit mass.

- Specific Power: The power of the battery per unit mass.

- Energy Density: The battery energy per unit volume.

- Power Density: The power of the battery per unit volume.

A LIB works when Li^+ ions flow from anode to cathode. Thus a net current flows from cathode to anode in the external circuit. The cell voltage is the highest in Lithium ion battery because of high reduction potential of lithium. A Lithium ion battery has three components namely – cathode, anode and electrolyte. A lithium ion battery works under two conditions [4]:

1. Charging: When charging is done Li^+ ions move from the cathode material to anode material.
2. Discharging: During discharging the Li^+ ions move from anode to cathode material.

The general electrochemical characteristics for a Lithium ion battery is shown in Figure 7 and Figure 8. Figure 7 shows the variation of specific capacity with charge/discharge cycles. Figure 5 shows the variation of the cell voltage with specific capacity.

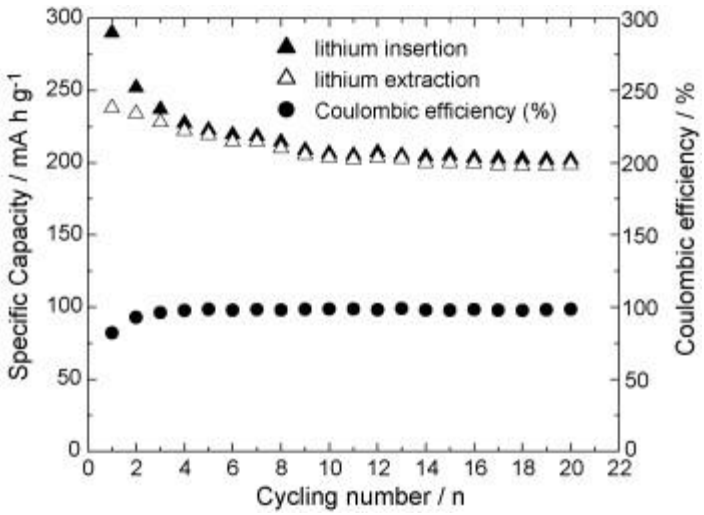

Figure 7: Electrochemical Property of Lithium ion battery [41]

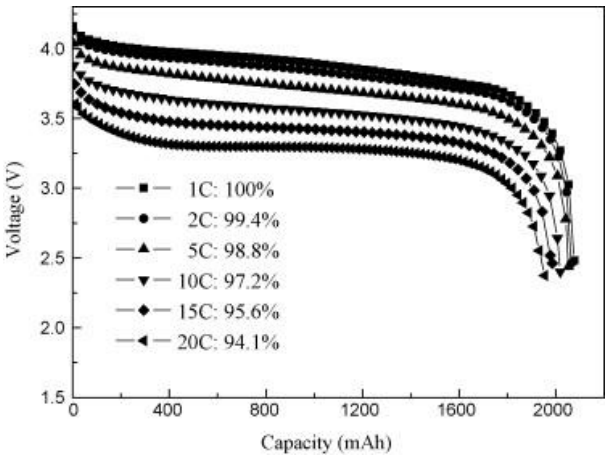

Figure 8: Cell Voltage Characteristics [40]

The characteristics features of Lithium ion batteries such as cell voltage, specific energy, specific power, cycle Life, cost etc. depend on the material properties of the cathode [18].

Lithium ion battery was introduced into the market in 1991-92. $LiCoO_2$ was used as cathode and graphite was used as anode.This set of cathode and anode has a cell voltage of around 3.6 Volt. The main disadvantage of $LiCoO_2$ is its toxic nature and its being expensive[19]. Some other compounds which are currently explored are $LiFePO_4$, $LiNiO_2$, $LiMn_2O_4$ and their composites. $LiNiO_2$ has the same structure as $LiCoO_2$ but it it could not be commercialized because of safety

concerns. With $LiMn_2O_4$ the cycle life and the thermal stability are the chief issues. While $LiFePO_4$ is a very promising cathode material because it is inexpensive, environment friendly, has good cycle stability, thermal stability, decent cell voltage around (3.5 Volts) and specific energy around 170 mAh g^{-1}. But the major disadvantage of $LiFePO_4$ is its low electrical conductivity (10^{-9} to 10^{-11} S cm^{-1}) and ionic conductivity (10^{-11} to 10^{-13} cm^2s^{-1})[10-19]. Efforts are being made to eradicate these problems in $LiFePO_4$ by [4, 5, 10-19]:

1. Coating $LiFePO_4$ with Conductive materials.
2. Decreasing the size of particles and making it mono-dispersed.
3. Doping with super-valent ions.
4. Improving the Morphology.

2.3.1.1 Coating $LiFePO_4$ with Conductive materials

The most common substance added to increase the conductivity and ionic diffusion coefficient of $LiFePO_4$ is Carbon. Adding Carbon into $LiFePO_4$ has many advantages. Carbon increases the electrical conductivity and ion diffusion coefficient of $LiFePO_4$, it acts as a reducing agent which prevents the oxidation of Fe^{2+}, and it also prevents the agglomeration of $LiFePO_4$ particles. Organic precursors such as citric acid, adipic acid, ascorbic acid, acetylene black, glucose, sucrose, polyethylene glycol etc. are used. Other metal coatings such as Copper and Silver have also been used [21-22].

2.3.1.2 Decreasing the size of mono-dispersed particle

Particle size has tremendous impact on the electrochemical properties of $LiFePO_4$. The relation between the diffusion time, diffusion distance and diffusion coefficient.

$$t = L^2/2D$$

t = diffusion time

L = diffusion distance

D= diffusion coefficient

According to this formula, the smaller of the particle size, the shorter diffusion time of lithium ions in $LiFePO_4$.Hence, resulting in a much enhanced electrochemical performances [19-21].

2.3.1.3 Doping with supervalent ions

$LiFePO_4$ can be doped in many ways. First way is to dope at Li sites, second way is to dope Fe sites, and third way is to dope O sites. By doing so we can significantly improve the properties of $LiFePO_4$.Table 3 shows a detailed analysis of the changes in properties due to different doping.

2.3.1.4 Improving the Morphology

Besides decreasing the particle size of $LiFePO_4$, its properties can also be improved by controlling its morphology. If the material has pores, then the electrode electrolyte interface increases and consequently the diffusion distance decreases. This helps in increasing the rate capacity of $LiFePO_4$.

Changes in properties of $LiFePO_4$ with the addition of dopants

S.R	Dopant	Cell Voltage	Cell Parameters	Particle Size	Ref.
1	Nickel	3.2V-3.4V	Life Cycle: 5500-7200	20 nm-60 nm	[25]
2.	Magnesium(Mg) & Cobalt (Co)	3.3V-3.4 V	High capacity retention	_	[26]
3.	Zinc	3.5 V	_	100 nm	[27]
4.	Manganese	3.25V-3.4V	_	_	[28]
5.	Magnesium	3.2 V-3.5V	Close to that of $LiFePO_4$	Micrometer range	[29]
6.	Niobium/C coat	3.3 V-3.4V	Band Gap - 0.08ev	50 nm-300 nm	[30]
7.	Vanadium	3.3 V	Higher Rate Capability	_	[31]
8.	Vanadium + VO_2 coating	3.2V-3.4 V	Increase in electronic conductivity	_	[32]
9.	Titanium	3.4V-3.5V	Good specific capacity	_	[33]
10.	Sodium & Titanium	3.4V-3.5V	Good cycle stability	_	[34]
11.	Chromium	_	Excellent Rate Performance	_	[35]
12	Zinc	3.5 V	Impedance is reduced	100 nm	[36]
13	Neodymium	3.5V	High initial Discharge Capacity	_	[37]
14	Fluorine	3.2V-3.4V	Narrow band Semiconductor 0.08 ev	_	[38]

Table 3: Change in properties of $LiFePO_4$ due to ion-doping.

2.3.2 Synthesis of $LiFePO_4$

$LiFePO_4$ can be synthesized by different methods. Each method has some advantages and disadvantages associated with it. Depending upon the synthesis process, different structure and characteristics are obtained. In this section a comparative study has been done. The main synthesis processes are:

1. Solid State Method
2. Microwave Method
3. Hydrothermal Method
4. Carbothermal Reduction
5. Sol-Gel Method

	Solid-state method	Sol–gel processing	Microwave processing	Hydrotheral reaction	Crabothermal reduction	Spray pyrolysis
Purity	Low	High	Moderate	High	High	High
Particle size	Digger	50–150 nm	40–50 nm	Bigger	100–300 nm	40–200 nm
Agglomeration	Yes	No	Yes	No	No	No
Complication degree of equipment	Simple	Simple	Simple	Complicate	Simple	Complicate
Reactive period	Long	Long	Short	Moderate	Long	Short
Energy consumption	High	Low	Low	High	High	Low
Reaction control	Easy	Easy	Difficult	Easy	Easy	Difficult
Industrialization	Easy	Difficult	Difficult	Difficult	Difficult	Difficult
Performance	Low	Good	Moderate	Moderate	Good	Moderate

Table 4: Comparison of different synthesis process [18]

2.3.2.1 Solid State Method

The solid state method is a simple and easy method for the synthesis of $LiFePO_4$. It is carried out at high temperature and pressure without any solvent. The particles formed by this method are

not very small and also has a poor electrochemical properties compared to other methods. For Lithium Li_2CO_3, $LiOH.H_2O$ and LiF are used. For iron source, $FeC_2O_4.2H_2O$, $Fe(C_2O_4)$ and

$Fe(CH_3CO_2)_2$and for Phosphorous group $NH_4H_2PO_4$ and $(NH_4)_2HPO_4$. In this method, particles are either mixed in a ball milling or manually. After mixing calcinations and then sintering is done. This method is easy to industrialize [18, 21].

2.3.2.2 Microwave Method

Microwave Method uses microwave radiation to synthesize cathode materials. The heating is done by microwave radiation at the molecular level. It takes time between 5 minutes to 20 minutes. It has short processing time. It is a low temperature process. It produces materi monodispersed particles. Carbon is used as microwave absorber. On prolonged heating , large particles are obtained as well as impurity such as Fe_2P are formed [20-24].

2.3.2.3 Hydrothermal Method

Hydrothermal Method is used for synthesis of cathode material in aqueous solution above the boiling point of the water. The whole synthesis is carried out inside an autoclave. Due to diffussion of particles is more in heated water, crystal growth is faster. The temperature of the autoclave is around 120 ^{0}C to 220 ^{0}C. The advantage of this method over other methods is that it is a low temperature method and does not require sintering. The disadvantage of this method is that carbon coating is not obtained. Hence , to obtain carbon coating, the sample has to be heated at high temperature with organic precursors [20-24].

2.3.2.4 Carbothermal Reduction

In carbothermal reduction, carbon is used as reducing agent to reduce Fe^{3+} to Fe^{2+} and also to prevent the oxidation of Fe^{2+}. Organic precursors such as Citric acid, Ascorbic Acid, Adipic Acid etc. are used as the carbon source. The calcination temperature is around 650 ^{O}C to 850 ^{O}C [20-24].

2.3.2.5 Sol-Gel Method

Sol Gel is a very simple method. It involves formation of colloidal suspension of solid particles in solvent known as sol. The gelation is done by the chelating agent such as citric acid or ascorbic acid. The chilating agent forms an interconnected structure with pores made up of sol particles. Because of this reason it is known as sol gel method. The sol gel is heated at 80 ^{O}C to form xerogel. The xerogel is then calcined at around 800 ^{O}C to form $LiFePO_4$.

Sol Gel Method has the following advantages:

1. It is a low cost method.
2. Reaction parameters, such as temperature, time, pH, precursor, solvent, concentration, and viscosity, etc., are of importance for the formation and ultimate morphology (particle size and shape, pore size, and porosity) of the obtained powders.

3. Sol Gel Method produces Micropores which increases the conductivity of $LiFePO_4$.
4. High purity, uniform structure and very small size is obtained.

Because of these advantages sol gel method has been chosen as the synthesis method by the author [20-24].

2.3.3 Structure of $LiFePO_4$

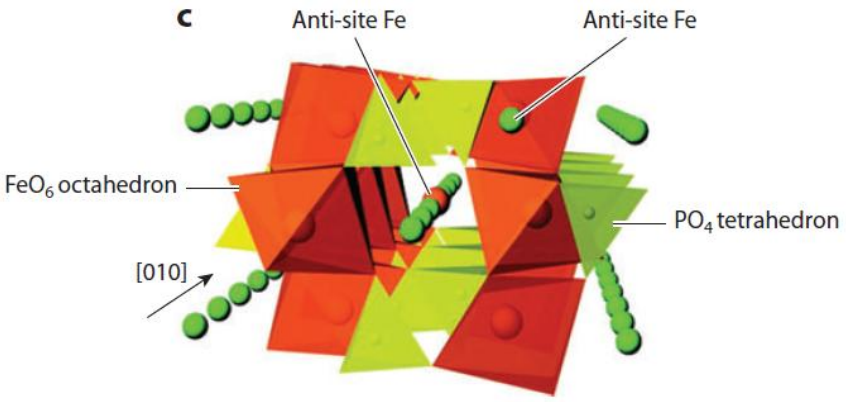

Figure 9: Crystal structure of $LiFePO_4$ [2]

$LiFePO_4$ has Olivine structure and Orthorhombic lattice structure. Li and Fe occupy octahedral void whereas P occupies tetrahedral voids. It can be seen from the diagram that Li^+ are free to move only in one direction [22].This is the reason for the low electrical conductivity of $LiFePO_4$.

2.3.4 Anode

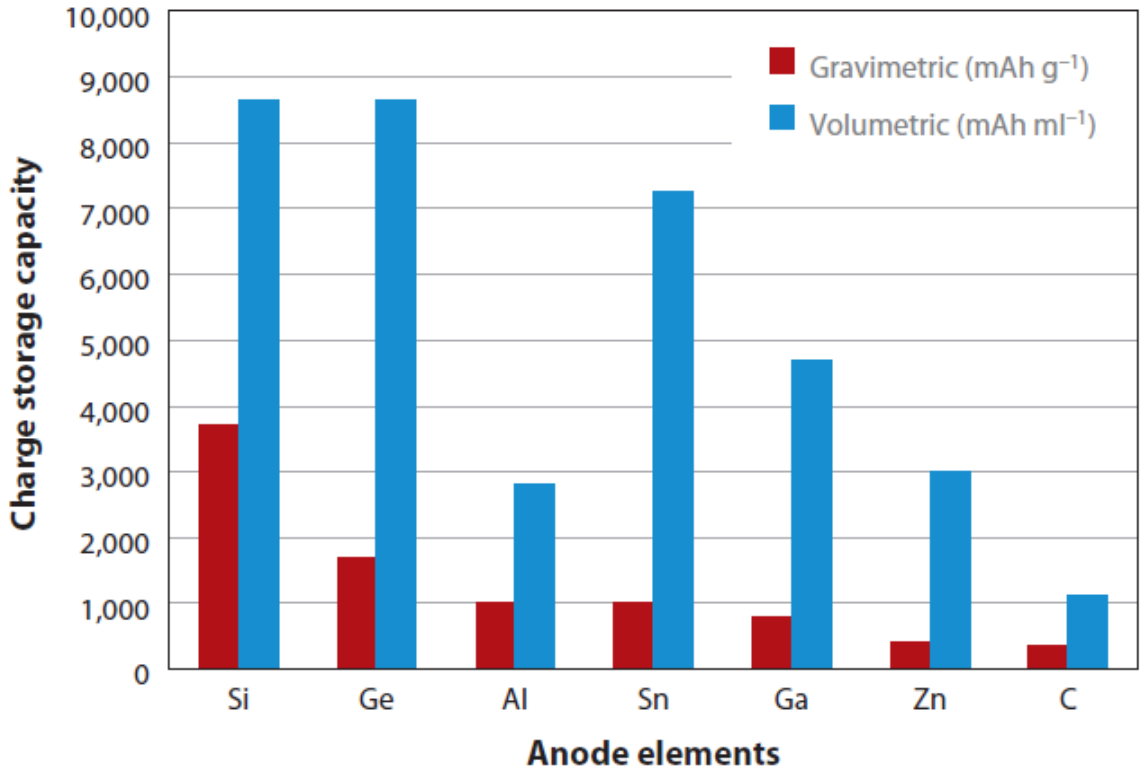

Figure 10: Comparison of anode material of Lib [22]

Commercially graphite is used as anode material along with $LiCoO_2$ as cathode material. Lithium insertion and extraction is easy in graphite. The lithiated compounds can form stable phase up to LiC_6. Its specific capacity is nearly 372 mAh g^{-1}. Tin and silicon compounds offer better specific capacity than conventional graphite anode. Transition metal oxide compounds also show very good insertion and extraction properties. These compounds have general formula MO where M is Cobalt, Nickel, Copper and Iron. The figure shows gravimetric density and volumetric density of some commonly used anode materials. From the above graph, it can be concluded that Silicon can be the best anode material. Due to continuous charge and discharge, the round trip voltage efficiency severely retards.

The anode materials can broadly be divided into:

I. Tin based materials.

Pure tin, tin/carbon composite, tin/cobalt, iron, titanium/carbon composite, tin oxide (tin oxide nanoparticles, tin oxide hollow structure, tin oxide nanotubes, tin oxide nanowire, tin oxide nanosheets), tin oxide/ carbon composites are materials

II. Silicon based materials.

Pure silicon, silicon/ carbon composite, binder based silicon materials are silicon based materials.

III. Graphite

2.3.5 Electrolyte

In commercially available LIB, a mixture of alkyl carbonates (DMC, EC, DEC, EMC) and $LiPF_6$ is used as electrolyte. Electrolytes give certain advantages [23]:

1. Good cycle Life.
2. Easy movement of Li+ ion from cathode to anode.
3. High discharge rate

Electrolytes are used in battery to enhance the performance of lithium ion battery. Its presence improves its cycle life. The main advantages of using additives to electrolytes are [24]:

1. Facilitate the formation of SEI (Solid Electrolyte Interface/ Interphase) on the surface of graphite.
2. Protect cathode from overcharge and dissolution.

3. Enhance the thermal conductivity of $LiPF_6$.
4. Protect cathode from dissolution and overcharge.
5. Improve the physical properties of electrolyte such as viscosity.

2.4 Optimization of $LiFePO_4$

The current situation demands the design of new cathode materials for Lithium ion battery which would provide high cell voltage, high life cycle, high specific energy, high power density and at the same time it has to be economical. It was found that $LiFePO_4$/C was suitable cathode material which can potentially replace $LiCoO_2$. But from our investigation of literature, it was found that nickel doped $LiFePO_4$ having general formula $LiFe_{1-X}Ni_XPO_4$/C ($0 \leq X \leq 1$) has the potential to fulfill the above criteria. We opted sol gel route which is one of the easiest and economical route for synthesis of these compounds.

Ge et all have reported that nickel doped $LiFePO_4$/C have very high life cycle around 5500 to 7200. On the other hand, $LiNiPO_4$ has very high cell voltage (5.1V). So, it is possible to optimize $LiFe_{1-X}Ni_XPO_4$/C ($0 \leq X \leq 1$) for a certain value of X that would fulfill all the above mentioned criteria [25].

Chapter 3: Experimental Methodology

3.1 Synthesis of $LiFePO_4$

Li_2CO_3, $NH_4H_2PO_4$, $Fe(NO_3)_3.9H_2O$ were taken in molar ratio of 0.5:1:1 and separately mixed in de-ionized water unless these were completely dissolved. Citric acid (weighing double the mass of Li_2CO_3, $NH_4H_2PO_4$, $Fe(NO_3)_3.9H_2O$ collectively) was also dissolved in de-ionized water. These four solutions were then mixed together and the pH of the mixed solution was maintained in between 5- 6 by adding NH_4OH solution. The resulting solution was heated at 80 ^{O}C in a magnetic stirrer unless a greenish yellow sol gel was formed. The sol gel was kept in a vacuum oven at 80 ^{O}C for 12 hrs to form xerogel. The xerogel was ground on a mortar unless powder is obtained. This powder was heated at 300 ^{O}C to dispel the volatile substances present in it. After this step, the powder was kept at 500 ^{O}C for 10 hrs in Argon environment and finally at 800 ^{O}C for 24 hrs in Argon environment. In this way, $LiFePO_4$ composite was obtained. The resultant product was characterized using X-Ray Diffractometer (XRD), Field Emission Scanning Electron Microscope (FESEM), and High Resolution Transmission Electron Microscope (HRTEM).

3.1.1 Synthesis of $LiFePO_4$ by Sol Gel Technique

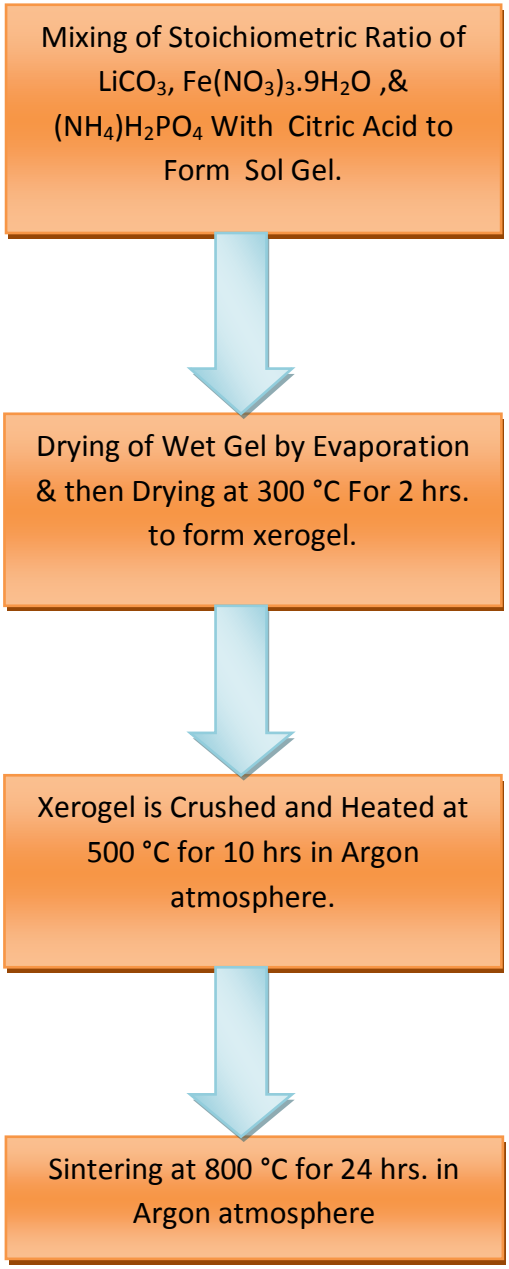

Figure 11: Synthesis process of $LiFePO_4$

3.2 Synthesis of $LiFe_{1-X}Ni_XPO_4$ (X= 0.125, 0.25, 0.375)

Li_2CO_3, $NH_4H_2PO_4$, $Fe(NO_3)_3.9H_2O$ & $Ni(NO3)_2.6H_2O$ were taken in molar ratio of 0.5:1:1-X:X and were separately mixed in de-ionized water unless they were completely dissolved. Citric acid (weighing double the mass of Li_2CO_3, $NH_4H_2PO_4$, $Fe(NO_3)_3.9H_2O$ & $Ni(NO3)_2.6H_2O$ collectively) was also dissolved in de-ionized water. These five solutions were then mixed together and the pH of the mixed solution was maintained in between 5- 6 by adding NH_4OH solution. The resulting solution was heated at 80 ^OC in a magnetic stirrer unless a sol gel was formed. The sol gel was kept in a vacuum oven at 80 ^OC for 12 hrs to form xerogel. The xerogel was ground on a mortar unless powder was obtained. This powder was heated at 300 ^OC to dispel the volatile substances present in it. After this step, the powder was kept at 500 ^OC for 10 hrs in Ar environment and finally at 800 ^OC for 24 hrs in Argon environment. Thus $LiFe_{1-X}Ni_XPO_4$/C composite was obtained. The resultant product was characterized using X-Ray Diffractometer (XRD), Field Emission Scanning Electron Microscope (FESEM), High Resolution Transmission Electron Microscope (HRTEM).

3.2.1 Synthesis of $LiFe_{1-X}Ni_XPO_4$ by Sol Gel Technique

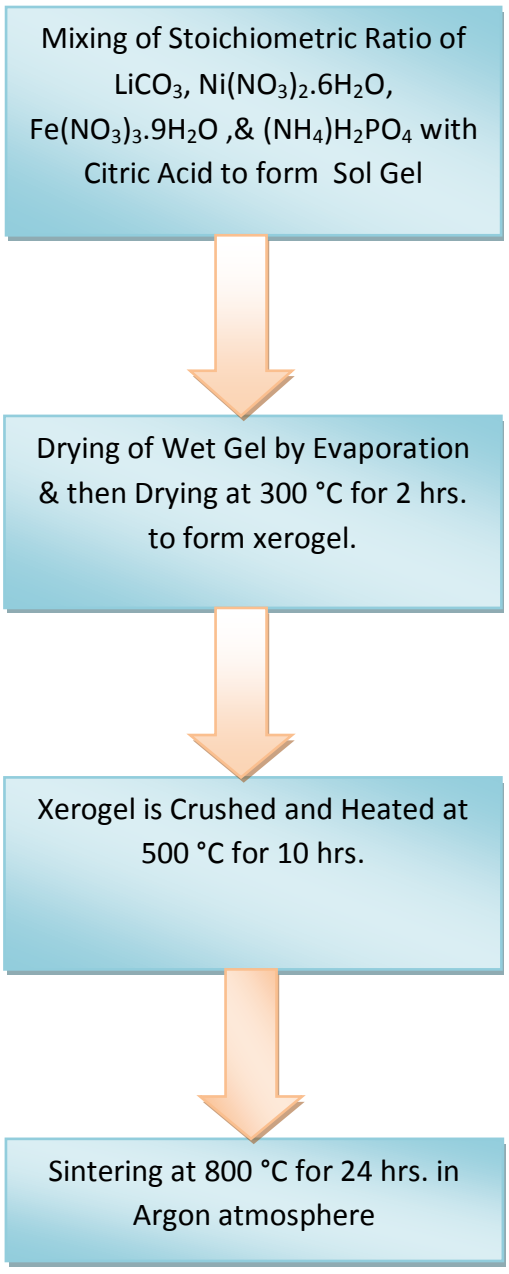

Figure 12: Synthesis of $LiFe_{1-X}Ni_XPO_4$

3.3 Experimental Setup

3.3.1 Magnetic Stirrer with Hot Plate

Figure 13: Magnetic stirrer with Hot Plate

The 'MLH' series magnetic stirrers with hot plate have additional stainless steel hot plate. PMDC motor gives higher torque even at lower speeds and maintains speed stability despite viscosity or volume changes. Accurate steeples speed control allows smooth variation up to 1200 rpm. Heating energy is controlled by energy regulator. Salient Features:

1. PMDC motor for higher torque even at low speeds
2. Better low speed stirring even with small volume
3. Accurate steeples speed control maintains excellent speed stability.

Li_2CO_3, $NH_4H_2PO_4$, $Fe(NO_3)_3.9H_2O$**/** Li_2CO_3, $NH_4H_2PO_4$, $Fe(NO_3)_3.9H_2O$ & $Ni(NO_3)_2.6H_2O$ were stoichiometrically mixed with de-ionized water and the resulting solution was mixed with a solution of

citric acid and deionized water. The pH was maintained between 5to 6. The final solution was stirred for 2 hrs to completely evaporate water.

3.3.2 Vacuum Oven

Figure 14: SNS SPAC-N-SERICE vacuum oven

The sol gel formed was kept in a SNS SPAC-N-SERICE vacuum oven at 80 ^{O}C for 12 hrs to obtain xerogel.

3.3.3 Mortar & Pestle

Figure 15: Mortar & Pestle

An agate mortar and pestle was used to grind xerogel into fine powder. Agate is a microcrystalline variety of SiO_2.

3.3.4 FurnaceAutomatic Temperature controlled Tube

Figure 16: Automatic Temperature Controlled Tube Furnace

The above experimental set up was used to perform calcinations and sintering. This set up consisted of an alumina tube, a furnace, a digital temperature controller, variac, relay, and ammeter, hydrogen and argon cylinder as well.

3.3.4.1 Alumina Tube

Alumina (Al_2O_3) has a high melting point around 2072 ^{O}C. It is used in furnace as a tube material.

3.3.4.2 Furnace

The furnace could go up to a maximum of 1000 ^{O}C.

3.3.4.3 Digital Temperature Controller

The required temperature in a digital temperature controller was adjusted manually. The controller had a thermocouple based sensor feedback system which sends a current signal proportional to the difference in temperature inside the furnace and outside the furnace. When the temperature difference becomes zero, it sends a signal to the relay and it switched off.

3.3.4.4 Relay

The relay was connected in between the variac and the furnace. It was also connected to the digital temperature controller. DTC sent signal to relay when specified temperature was obtained. In this way the relay was working as a switch.

3.3.4.5 Variac

The variac gave output voltage in between 0 to 260 Volts for 240 Volt input supply.

The powdered xerogel was heated at 300 ^{O}C in open environment for 2 hrs, followed by 500 ^{O}C in Argon environment for 10 hrs and 800 ^{O}C in Ar(90% by volume)/H_2(10% by volume) atmosphere for 24 hrs.

3.3.5 Gas leak Detector

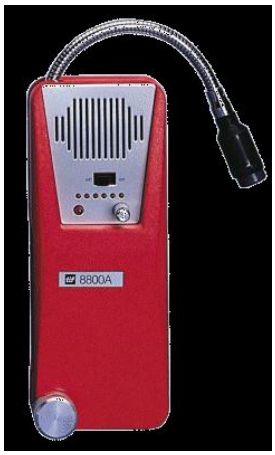

Figure 17: Gas Detector

This Combustible Gas Detector Audible and Visual Leak Size Indicators give us the response we want whenever there is any leakage of combustible gas. As a combustible gas or vapor source is approached, a **"Geiger counter"** Signal increases in frequency and the red lights illuminate in sequence, to show the intensity of the leak. Then you can see and hear your way to pin pointing dangerous leaks. We have to continuously monitor the setup if there is any leakage from any joints or near the furnace and if we get the alarm signal then immediately turn of the main power source and the gas supply to avoid any kind of accident.

3.3.6 X-Ray Diffractometer

Figure 18: Bruker D8 Advance X-Ray Diffractometer

Powder sample of $LiFePO_4$ & $LiFe_{1-X}Ni_XPO_4$ composites were verified by Bruker D8 Advance X-Ray Diffractometer using Cu-Kα radiation (λ=1.54 Å). The X-ray Source is a 2.2kW Cu anode long fine focus ceramic X-ray tube. The running conditions for the X-Ray tube are 40 kV and 40 mA, the power supply controls these with a stability of better than 0.01% for the high voltage and 10% of the variation of the supply for the current. Continuous scanning was carried out over the diffraction angle 2θ in the range $0° < 2\theta < 50°$ with a step size of 0.02°.

3.3.7 Field Emission Scanning Electron Microscope

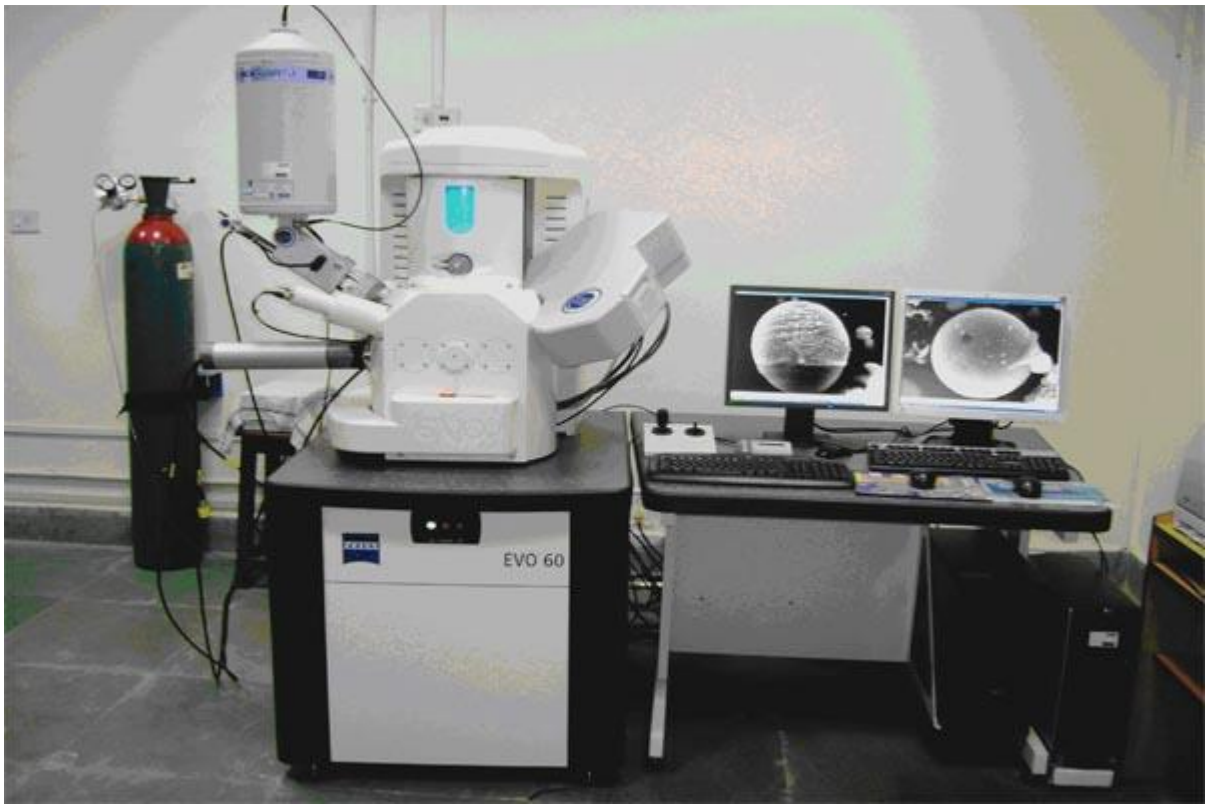

Figure 19: Carl Zeiss Field Emission Scanning Electron Microscope

ZEISS Sigma HD Field Emission Scanning electron microscope (FE-SEM), as shown in Figure with Oxford EDS detector has been used for micro structural characterization of the powder sample of $LiFePO_4$ composite. The Microscope works with tungsten filament and maximum acceleration voltage of 30 kV. The images are collected at selective scales of magnifications aiming to resolve the surface features giving a clearer picture of the small $LiFePO_4$ & $LiFe_{1-X}Ni_XPO_4$ particles embedded.

3.3.8 High Resolution Transmission Electron Microscope

Figure 20: JEOL JEM -2100 High Resolution Transmission Electron Microscope

The detailed micro structural characterization of the powder sample was carried out using JEOL JEM – 2100 High Resolution Transmission electron microscope. For preparation of the specimen for the TEM studies, the powders are mixed with acetone and a solution is made. The electron microscope is operated at accelerating voltage of 200 kV and analysis was carried out with a LaB6 filament. It has point to point resolving power of 0.194 nm fitted with energy dispersive spectrometer for chemical analysis. Bright field images, dark field images and selected area diffraction patterns of the specimen are recorded and analyzed.

Chapter 4: Result & Discussion

4.1 Experimental Analysis of $LiFePO_4$

The X-Ray diffraction patterns (Figure 21) were analyzed using X'Pert High Score Plus software. The X-Ray Diffraction image of the LiFePO4/C samples show that crystalline $LiFePO_4$ is formed. The XRD pattern matches with the PDF Reference Code: 00-019-0721. Carbon peaks are not detected in this case, indicating the presence of either extremely low crystalline carbon or completely amorphous carbon. Figure 27 shows EDAX analysis of different regions the material as seen under FESEM. Carbon was found in some of the regions. Hence, the above XRD pattern confirms the formation of $LiFePO_4$/C composite.

The Crystallographic parameters of $LiFePO_4$ as revealed from analysis using X'Pert High Score are as follows:

Crystal System: Orthorhombic

Space group: Pmnb

Space Group Number: 62

a = 5.99 Å
b = 10.31 Å
c = 4.68 Å
α = 90°
β = 90°
γ = 90°

Calculated Density = 3.62 g/cm^3
Volume of the cell = 10^6 pm^3

The Crystallite sizes as calculated by the X'Pert High Score Software corresponding to the major peaks in the sample are as follows:

S.R.	Bragg's Angle(°Θ_B)	FWHM(Θ_B radian)	d_{hkl}(Å)	Crystallite Size (nm)
1.	10.4826	0.0000745364235	4.23388	237.41
2.	12.8745	0.0000745364235	3.45710	233.47
3.	14.9608	0.00158688	2.98382	10.97
4.	17.8972	0.0009918	2.50679	18.44

5.	26.3508	0.000801444	1.73543	24.22

Table 5: Crystallite Size Calculation

The Average Crystallite Size of $LiFePO_4$ corresponding to four major peaks is: 104.902 nm.

$LiFePO_4$ sample was gold coated and observed in Carl Zeiss Sigma Field Emission Scanning Electron Microscope. The FE-SEM images showed magnified images of crystal grains and the presence of carbon around the grains at some places. The $LiFePO_4$ formed was porous. It had micro pores and nano pores. The average grain size was found to be 0.675 µm. The order of magnitude of this matches with that inferred from XRD peaks. However, the value of is more 0.675 µm reliable.

The EDS data showed that atomic percentage of Iron (Fe) and Phosphorous (P) was almost equal and the atomic percentage of Oxygen (O) was almost four times the atomic percentage of iron and phosphorous. Lithium being a very light element could not be detected in EDS analysis.

Hence the EDS Analysis confirms the formation of $LiFePO_4$.

S. N.	Particle Size (µm)	S. N.	Particle Size (µm)
1.	1	7.	1.23
2.	1.27	8.	0.23
3.	0.48	9.	0.68
4.	0.38	10.	0.71
5.	0.16	11.	1.08
6.	0.52	12.	0.36

Table 6: Grain Size Distribution of $LiFePO_4$

High Resolution Transmission Microscope Images show the presence of $LiFePO_4$ and carbon around it. Selected area diffraction (SAD) Images were taken at different portion of the sample. Figure 31 (b) shows very distinct concentric circles indicating the presence of fine grained polycrystalline $LiFePO_4$. Figure 31 (d) and Figure 32 (c) show the presence of single crystal as well as mixed amorphous material. It is due to the presence of single crystal $LiFePO_4$ and amorphous carbon. The interplanar distance calculated from the Lattice Fringe Pattern (Figure 33) is 3.33 °A. From PDF Reference Code : 00-019-0721 (JCPDS), the family of planes corresponding to inter planar distance 3.33 °A comes out to be **(211)**.

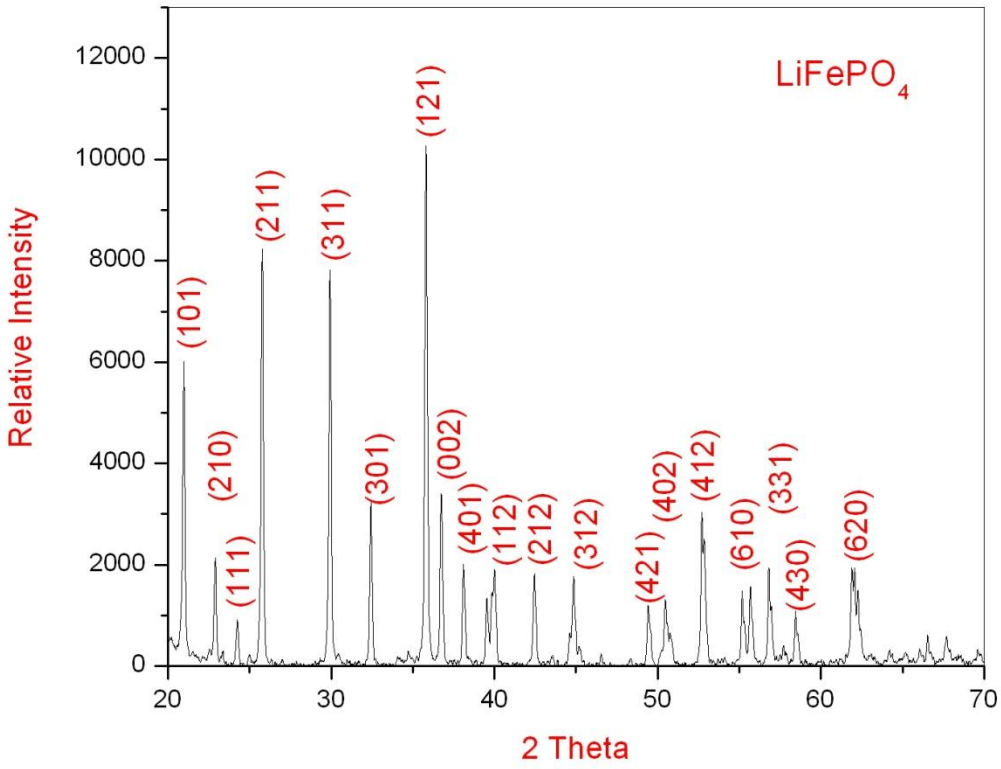

Figure 21: XRD Image of $LiFePO_4$

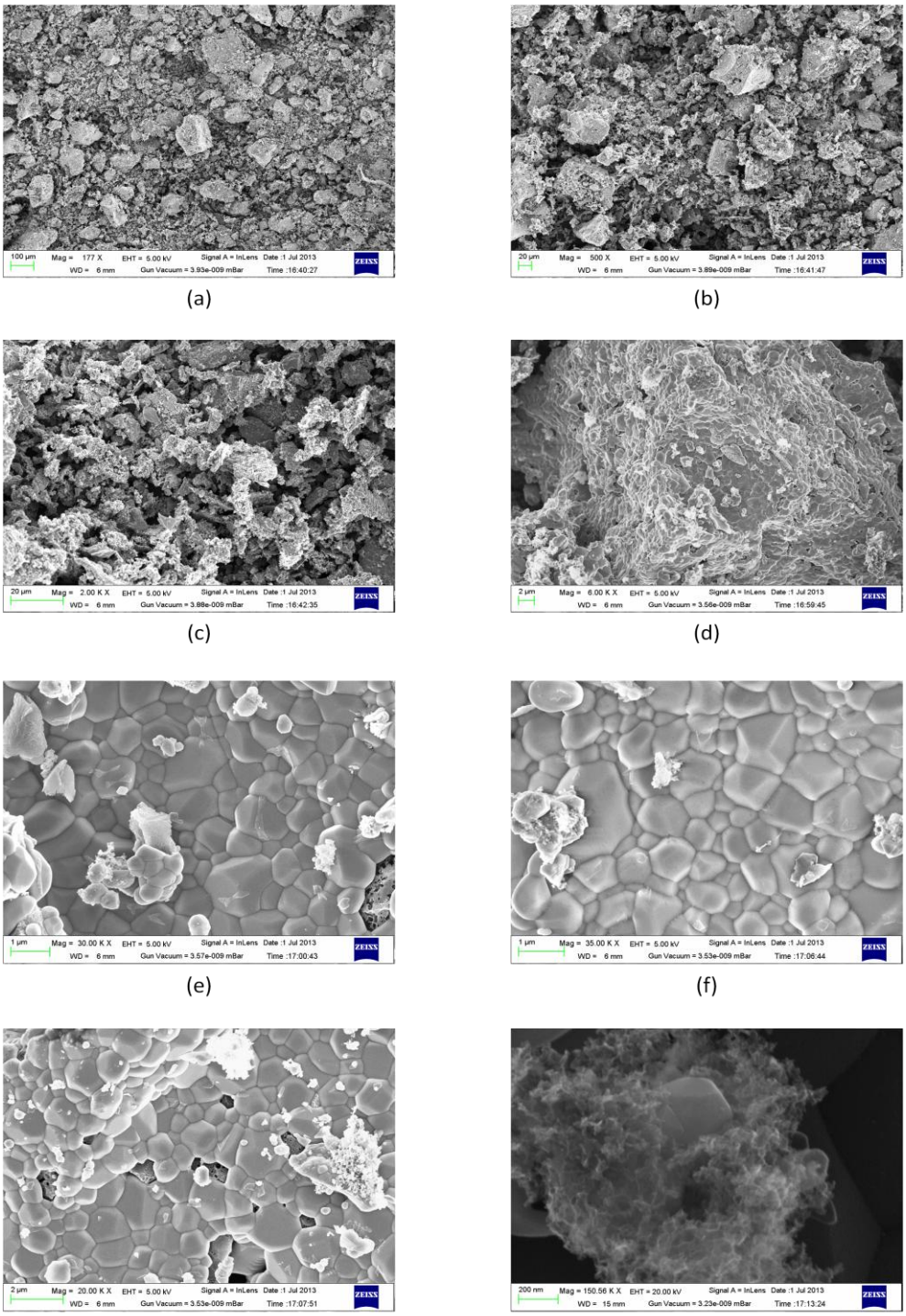

Figure 22: FE-SEM Images of $LiFePO_4$ at different magnifications

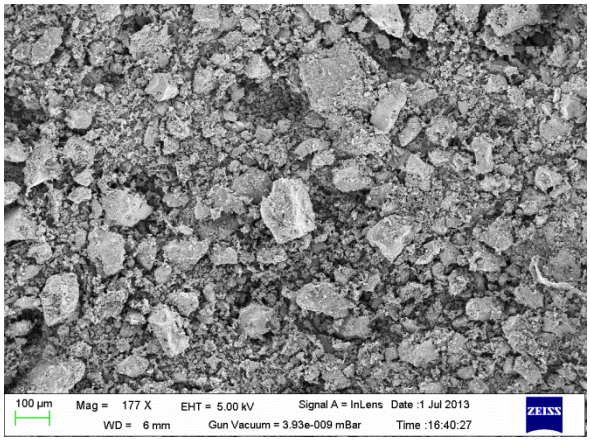

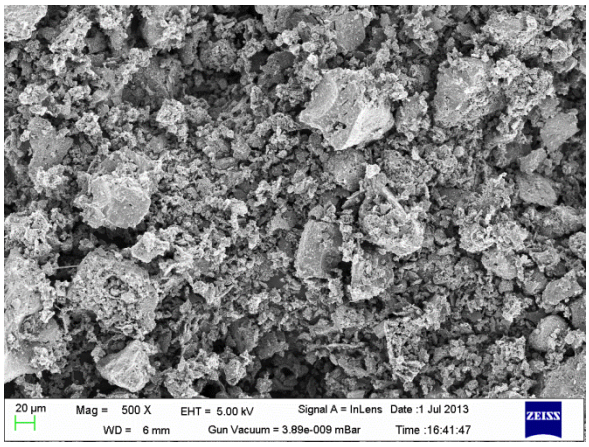

Figure 23: $LiFePO_4$ micro range clusters

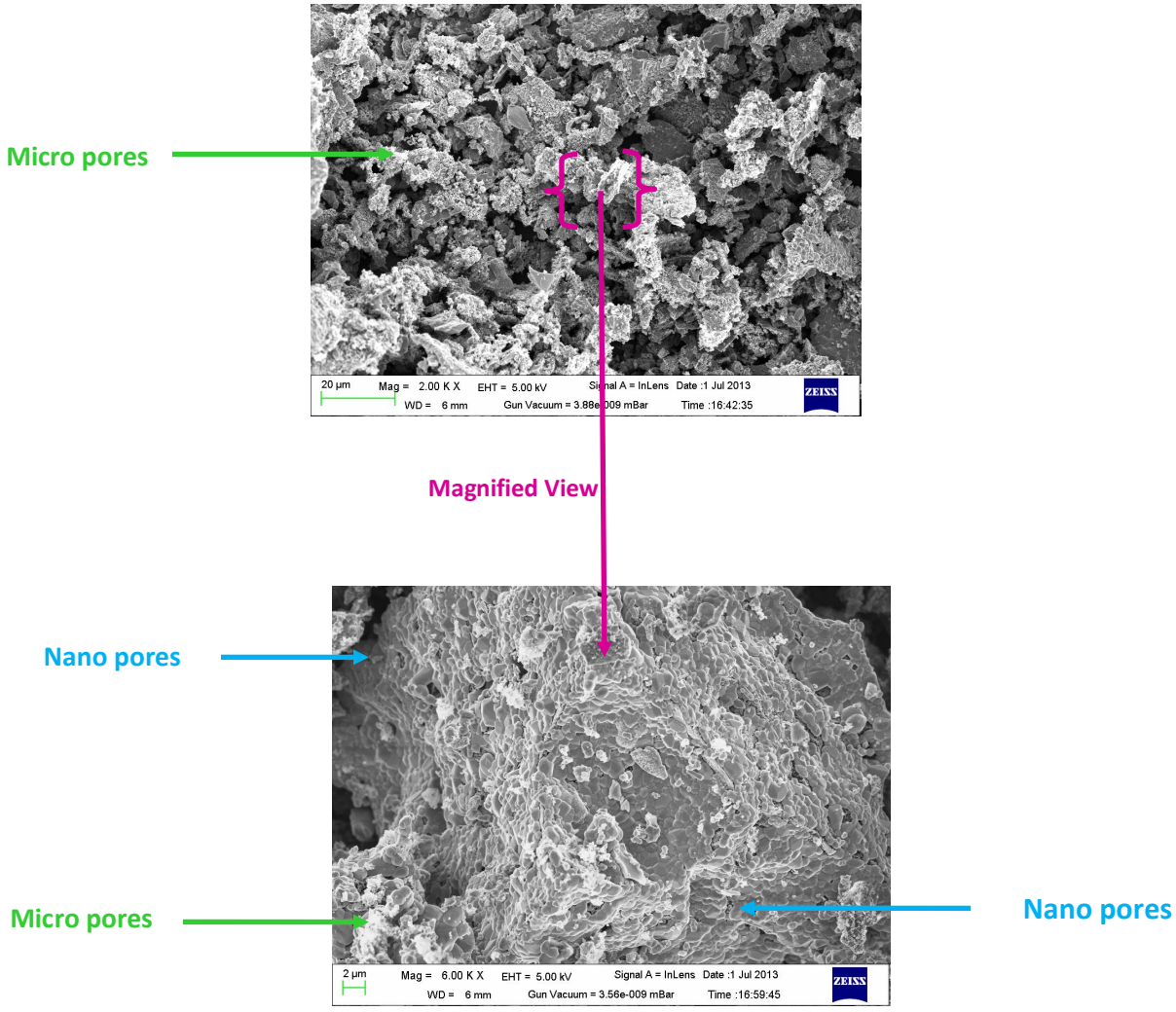

Figure 24: Magnified View of $LiFePO_4$ agglomerate

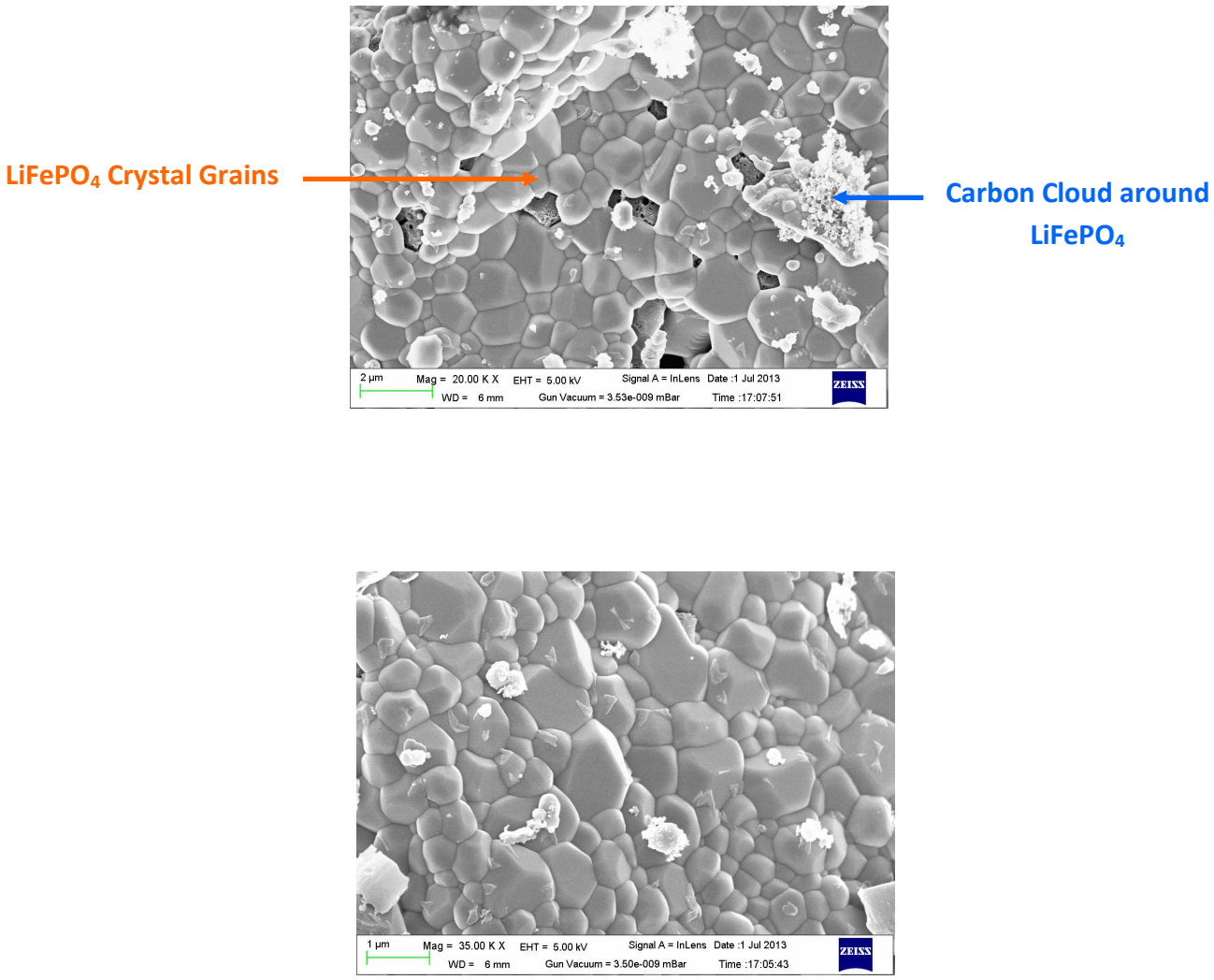

Figure 25: $LiFePO_4$ Crystal Grain & Carbon

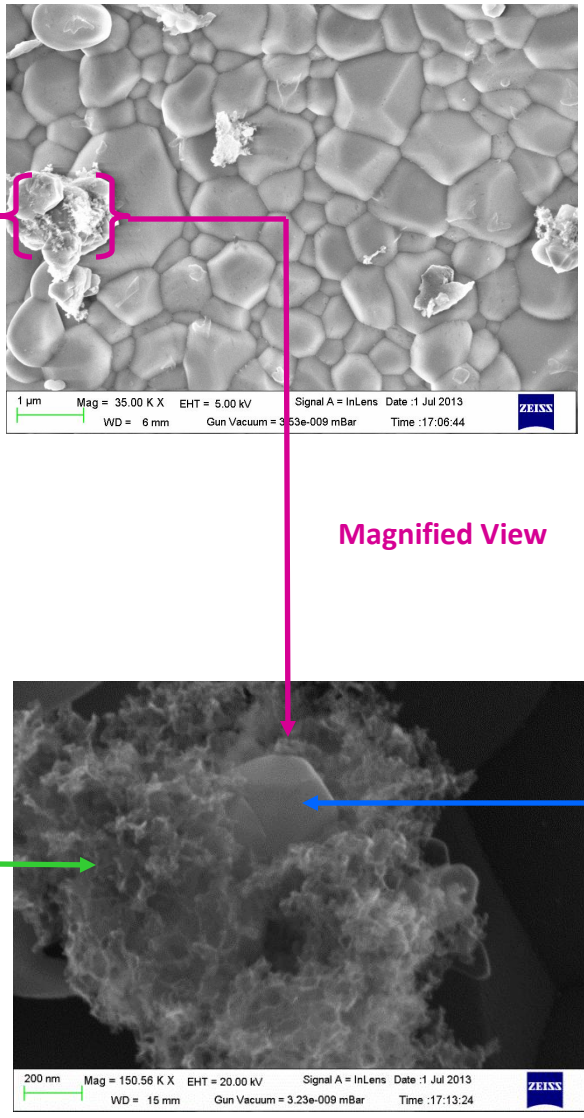

Figure 26: $LiFePO_4$ Crystal Grain & Carbon

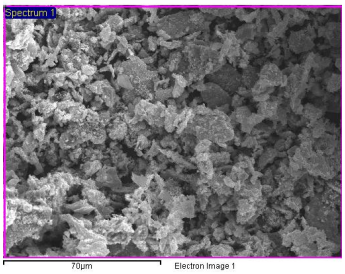

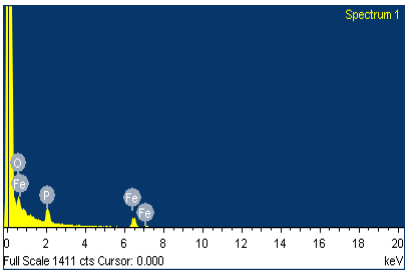

Element	Weight%	Atomic%
C K	0.00	0.00
O K	36.48	61.74
P K	19.14	16.73
Fe K	44.38	21.52
Totals	100.00	

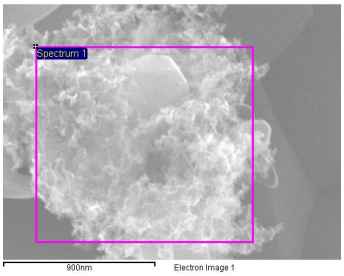

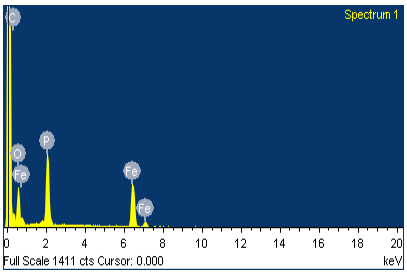

Element	Weight%	Atomic%
C K	19.50	34.62
O K	31.46	41.93
P K	15.40	10.60
Fe K	33.64	12.84
Totals	100.00	

Figure 27: EDS of $LiFePO_4$ at different magnification

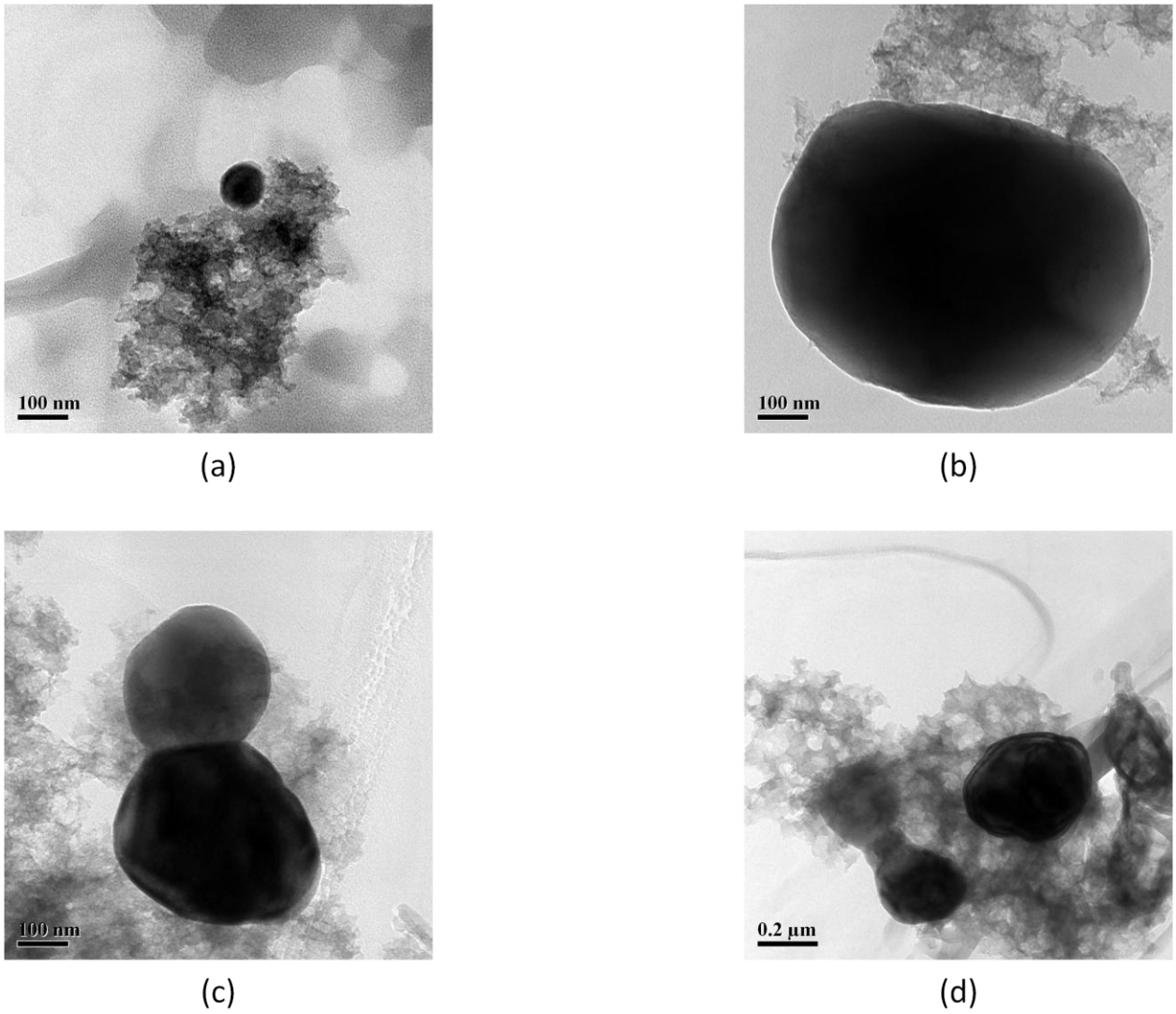

Figure 28: HR-TEM Micrographic Images of $LiFePO_4$

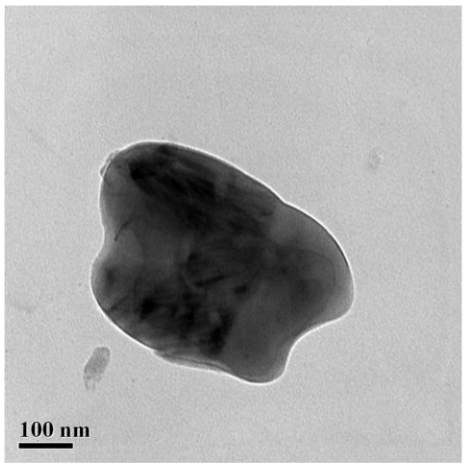

(e)

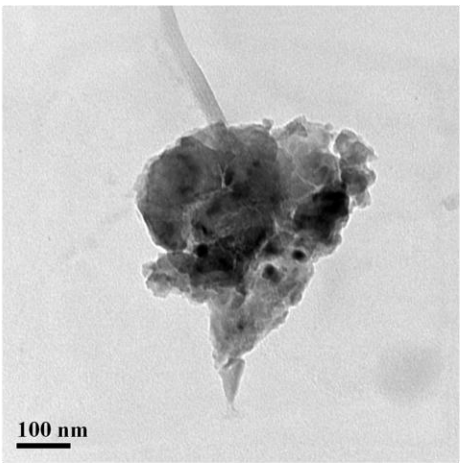

(f)

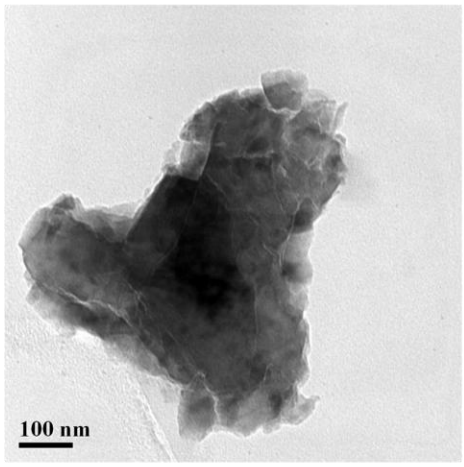

(g)

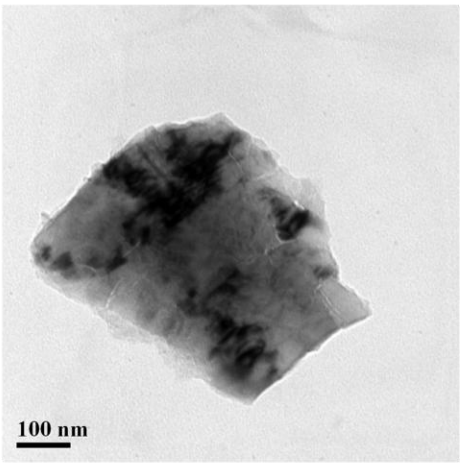

(h)

Figure 29: HR-TEM Micrographic Images of $LiFePO_4$

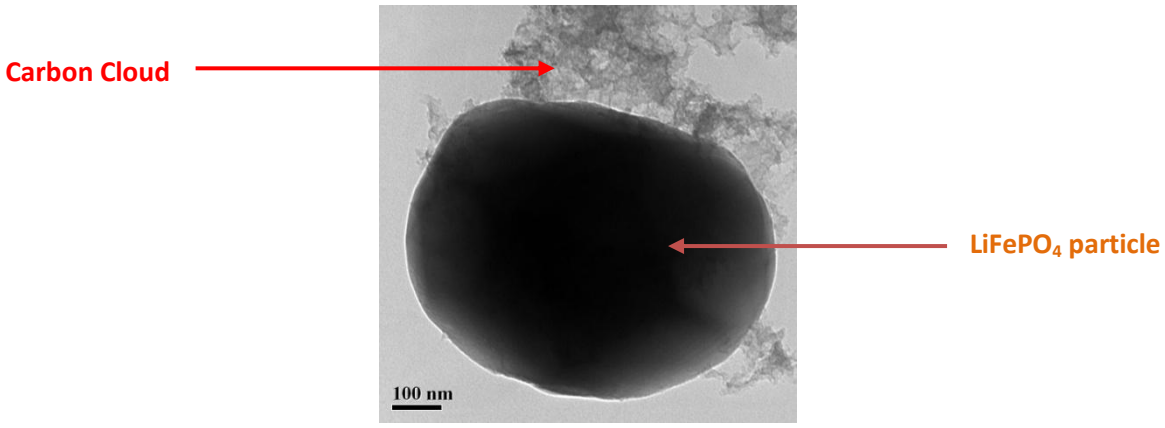

Figure 30: $LiFePO_4$ particle and carbon cloud

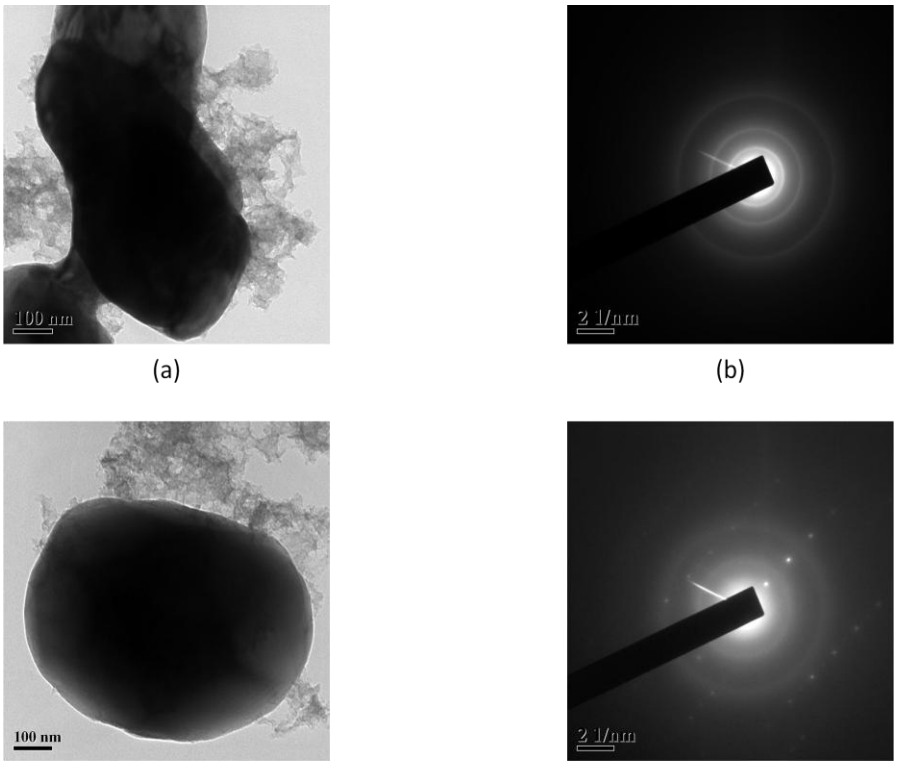

(a) (b)

(c) (d)

Figure 31: SAD Images of the $LiFePO_4$ Micrograph

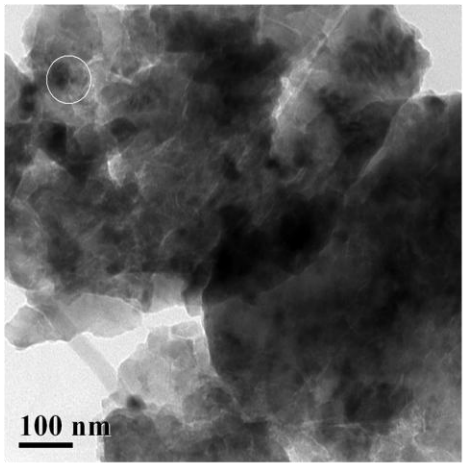

(a) Image of $LiFePO_4$

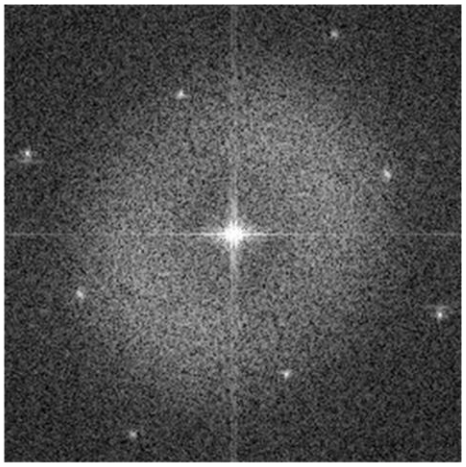

(b) Live FFT View

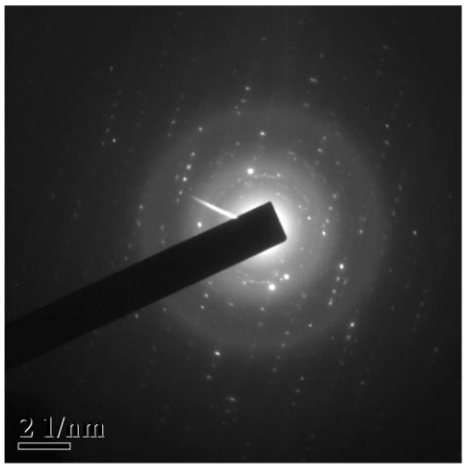

(c) SAD Image

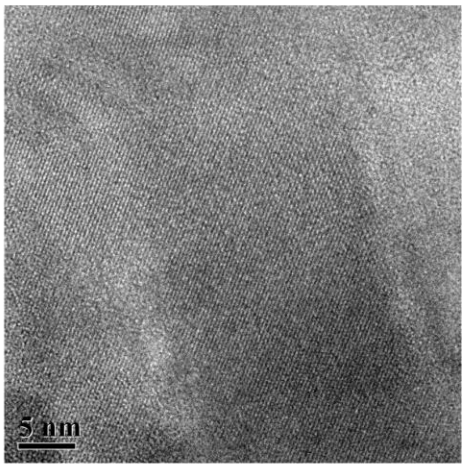

(d) Lattice Fringe Image

Figure 32

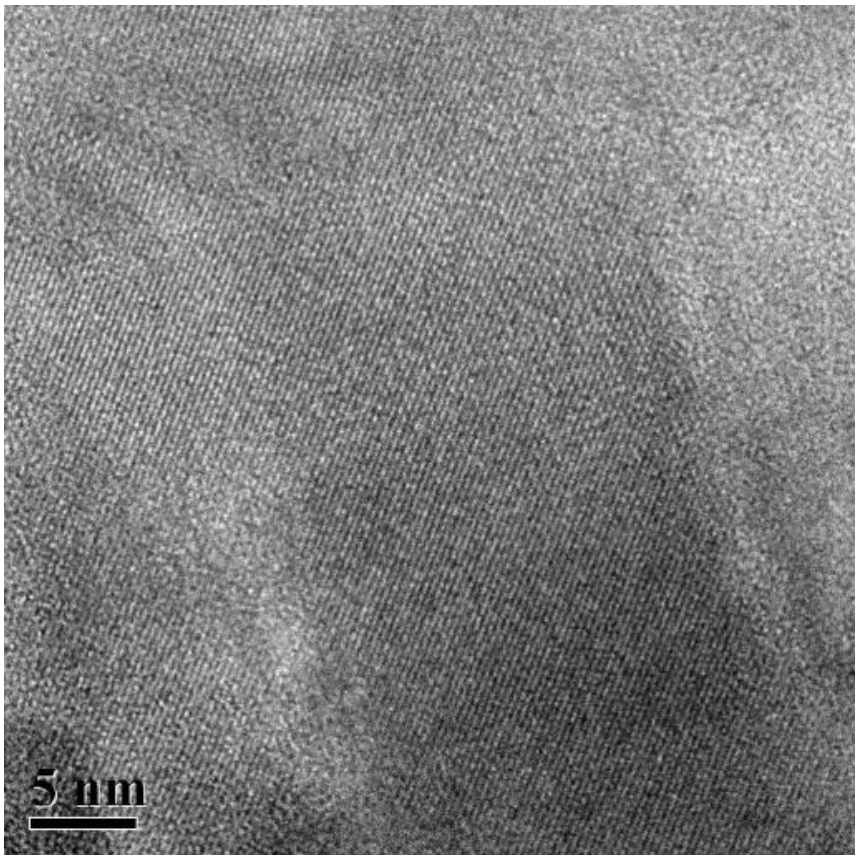

Figure 33: Lattice Fringe Pattern of $LiFePO_4$

4.2 $LiFe_{0.875}Ni_{0.125}PO_4$

The XRD pattern shows that crystalline $LiFe_{0.750}Ni_{0.250}PO_4$ was formed. The XRD peaks closely matched (extremely low shift) the peaks of $LiFePO_4$. This shows that 12.5 % doping of Nickel was successful. Along with crystalline grains, regions of different morphology having Iron, Nickel, Phosphorous and Carbon was also formed. This is evident from the FE-SEM images.

S.N.	Particle Size(μm)	S.N.	Particle Size(μm)
1	3.33	6	2.775
2	2.775	7	2.553
3	1.554	8	2.22
4	1.998	9	2.22
5	1.332	10	1.998

Table 7: Grain Size Distribution of $LiFe_{0.875}Ni_{0.125}PO_4$

The average grain size calculated is: 2.22 μm.

The EDS Data showed that the composition close to $LiFe_{0.875}Ni_{0.125}PO_4$ was obtained when EDS of grains were done. Whereas at other positions, atomic ratio between the elements was not maintained.

The HR TEM image showed Lattice Fringes at 5 nm scale. SAD pattern in Figure 39 (h) shows that the material has less number of grains compared to $LiFePO_4$. This is true because FESEM image confirms the formation of amorphous mixture of Nickel, Iron, Phosphorous and Carbon.

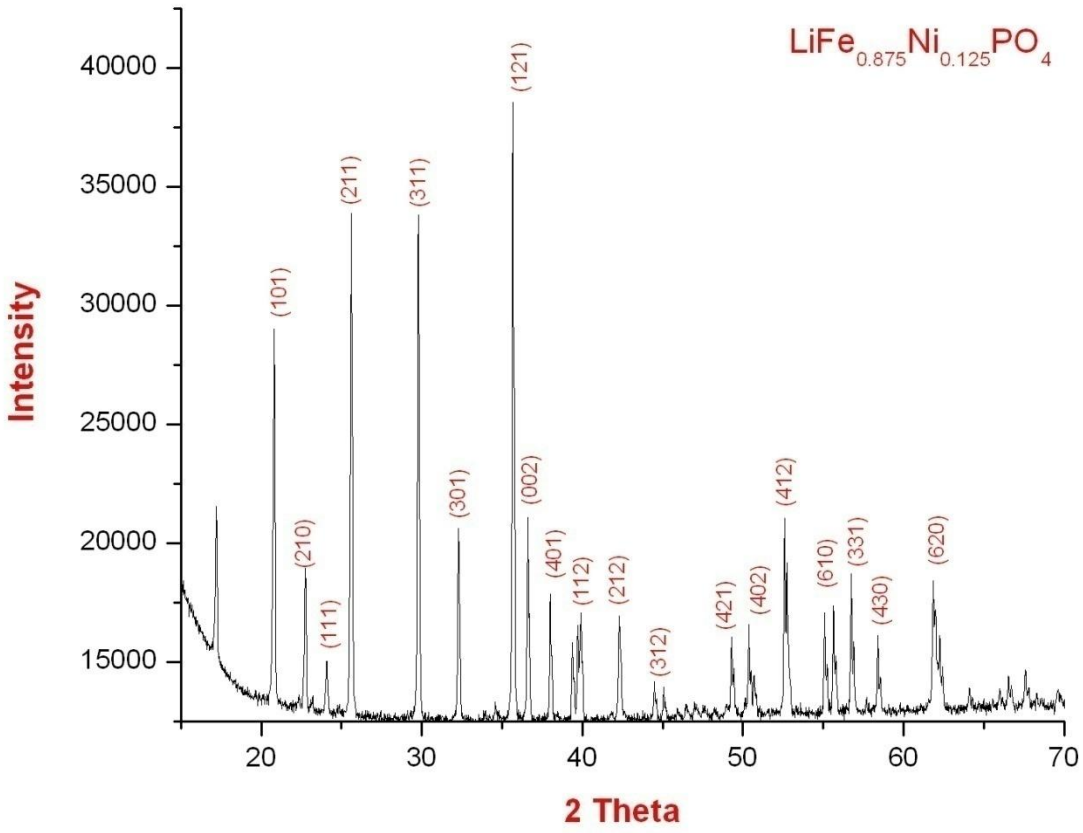

Figure 34: XRD Image of $LiFe_{0.875}Ni_{0.125}PO_4$

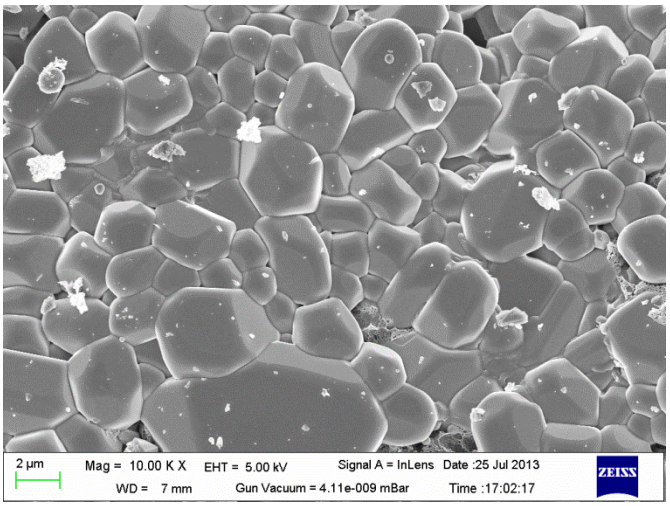

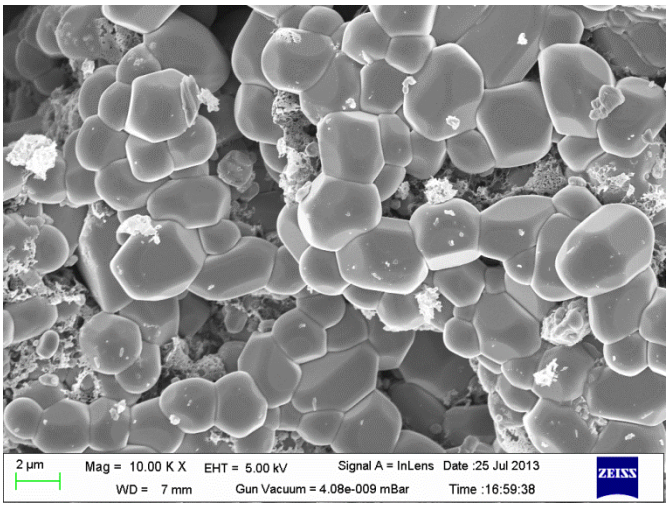

Figure 35: $LiFe_{0.875}Ni_{0.125}PO_4$ Grain Images

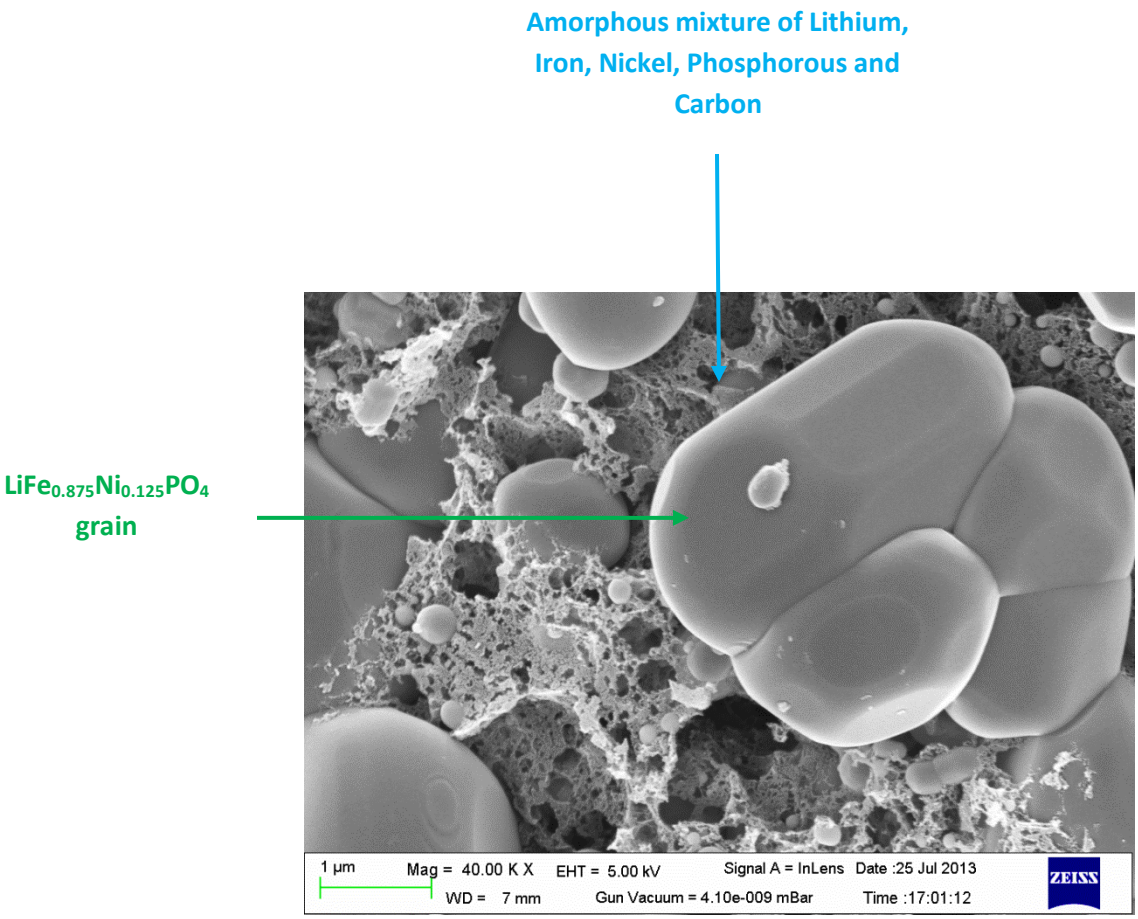

Figure 36: $LiFe_{0.875}Ni_{0.125}PO_4$ grains and amorphous mixture

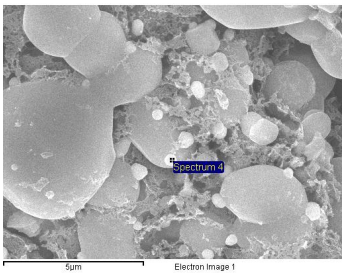

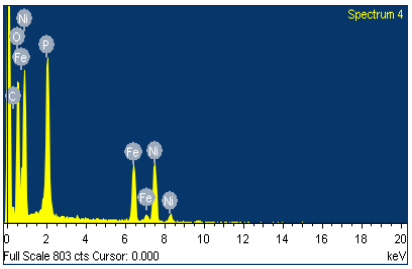

Element	Weight%	Atomic%
C K	11.44	22.36
O K	34.88	51.16
P K	13.17	9.98
Fe K	14.93	6.27
Ni K	25.58	10.23
Totals	100.00	

Figure 37: EDS Data of $LiFe_{0.875}Ni_{0.125}PO_4$

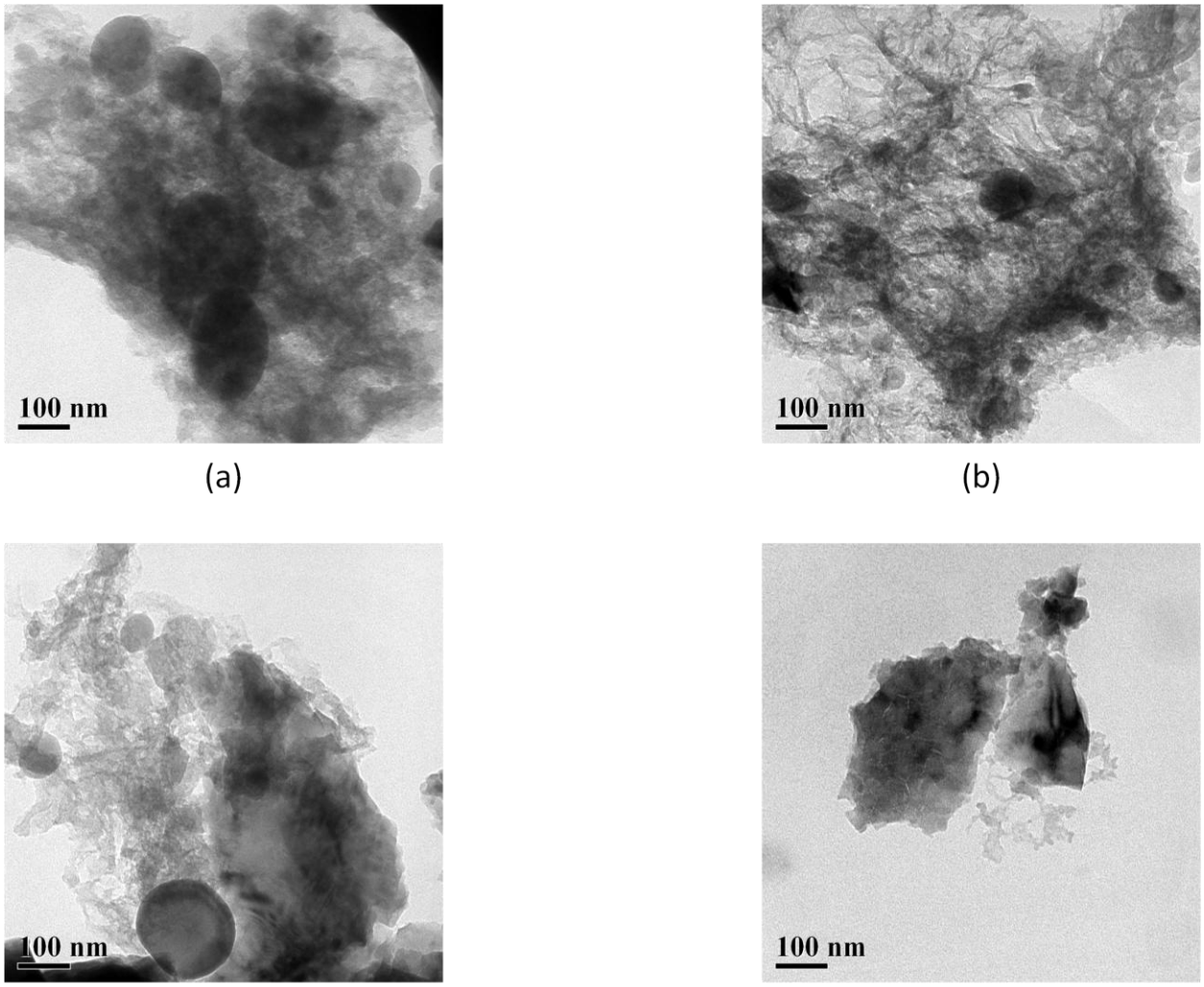

Figure 38: HR-TEM Micrographic Images of $LiFe_{0.875}Ni_{0.125}PO_4$

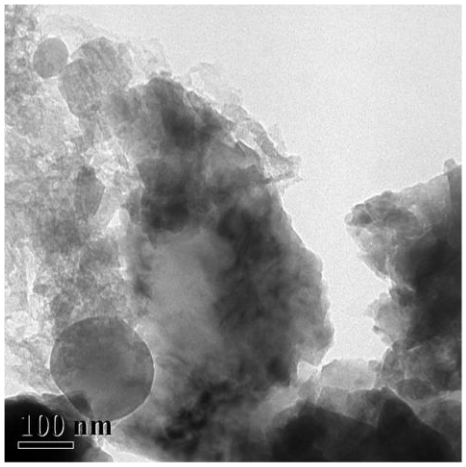

(e)

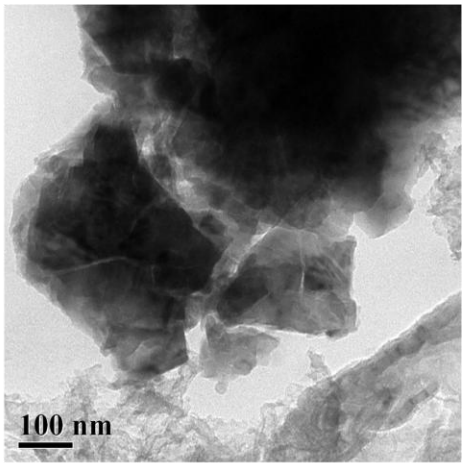

(f)

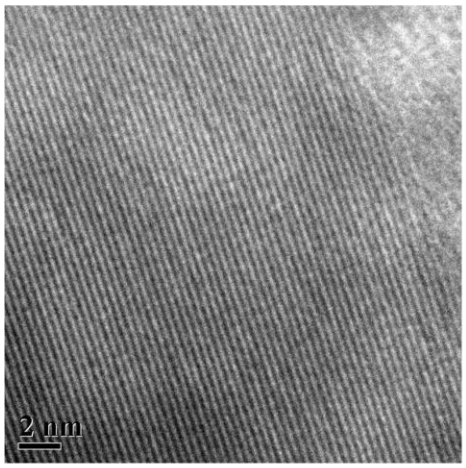

(g)

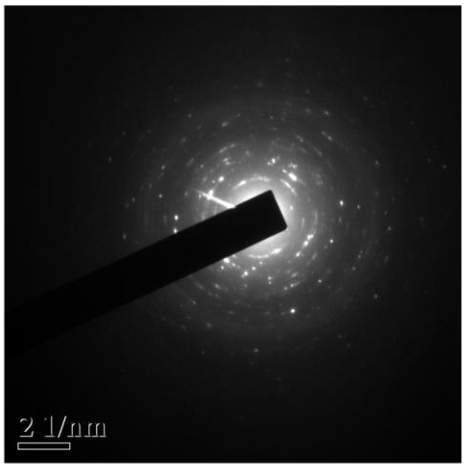

(h)

Figure 39: HR-TEM Images of $LiFe_{0.875}Ni_{0.125}PO_4$

4.3 $LiFe_{0.750}Ni_{0.250}PO_4$

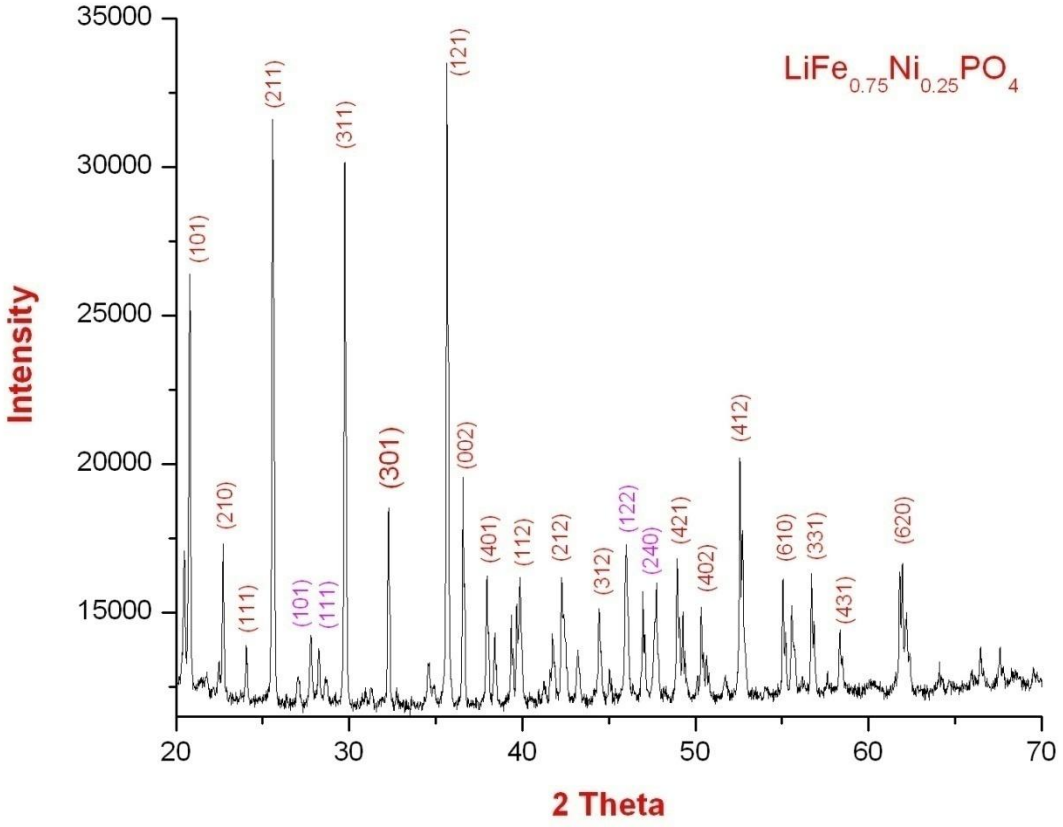

Figure 40: XRD Image of $LiFe_{0.75}Ni_{0.25}PO_4$

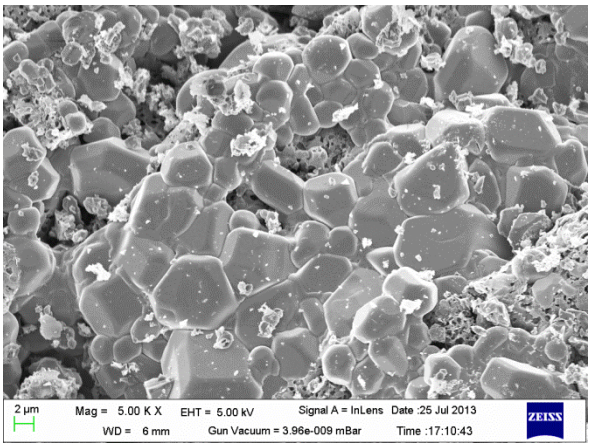

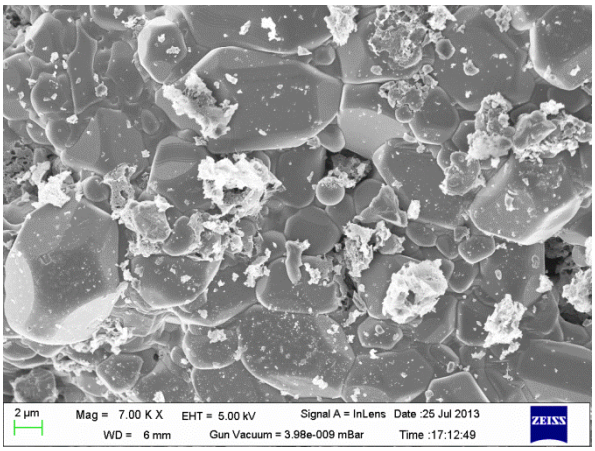

Figure 41: $LiFe_{0.750}Ni_{0.250}PO_4$ Grain Images

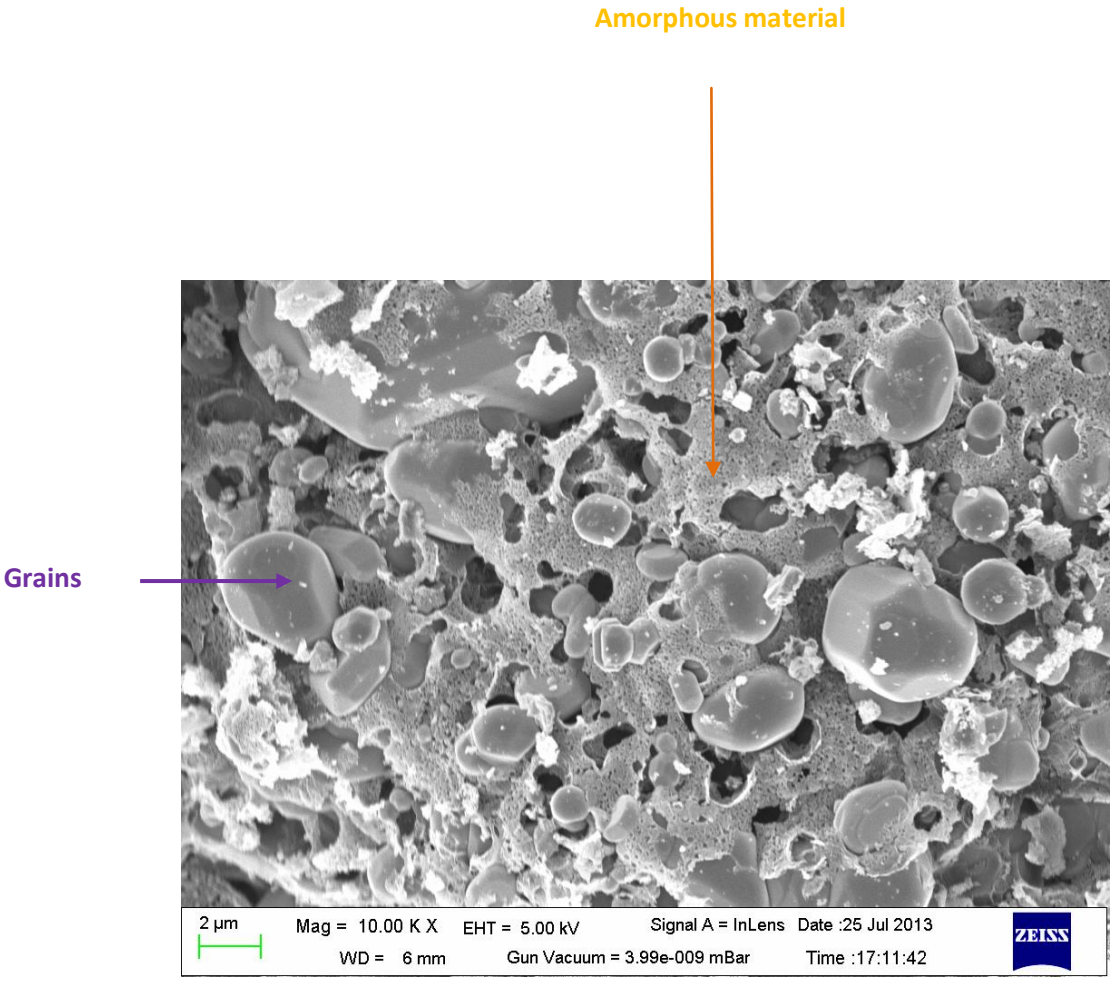

Figure 42: Grains and amorphous mixture of $LiFe_{0.750}Ni_{0.250}PO_4$

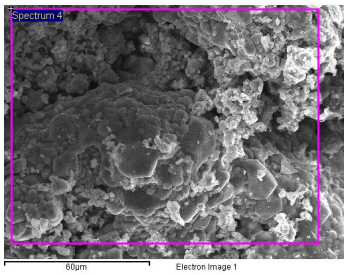

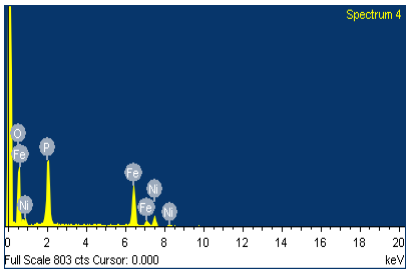

Element	Weight%	Atomic%
O K	38.04	63.76
P K	17.54	15.19
Fe K	32.29	15.51
Ni K	12.14	5.55
Totals	100.00	

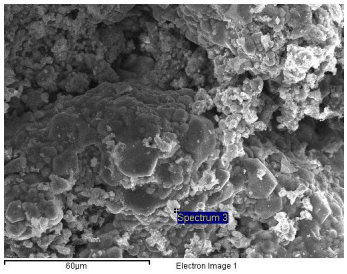

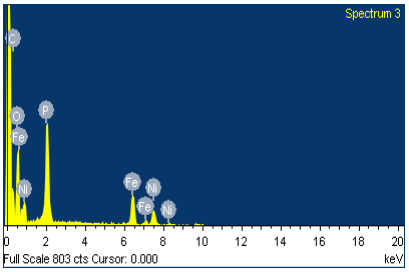

Element	Weight%	Atomic%
C K	32.06	46.89
O K	37.36	41.01
P K	10.30	5.84
Fe K	12.26	3.86
Ni K	8.02	2.40
Totals	100.00	

Figure 43: EDS Analysis of $LiFe_{0.750}Ni_{0.250}PO_4$

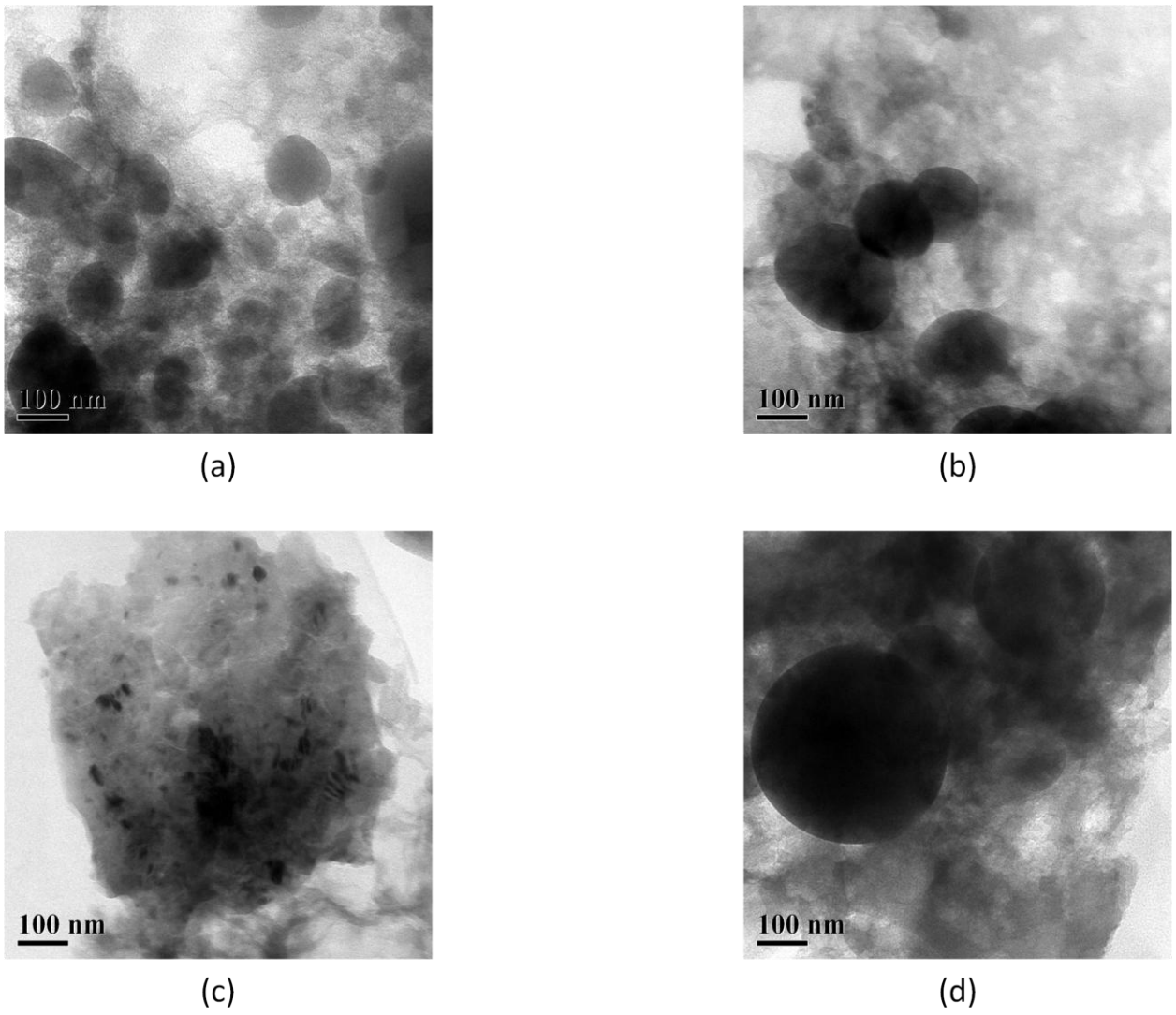

Figure 44: HRTEM Images of $LiFe_{0.750}Ni_{0.250}PO_4$

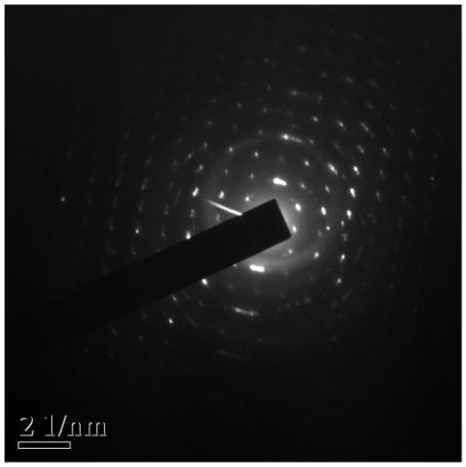

(e)

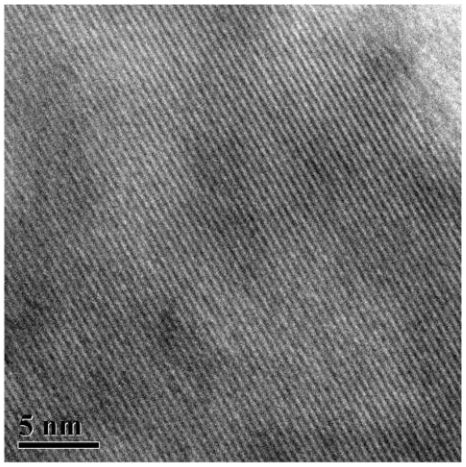

(f)

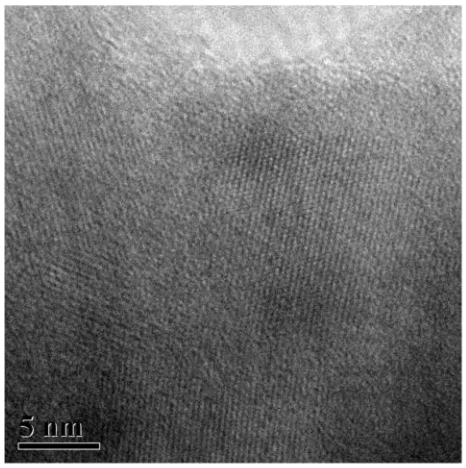

(g)

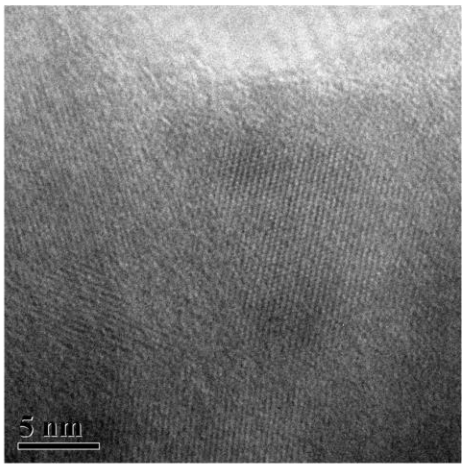

(h)

Figure 45: SAD & Lattice Fringes of $LiFe_{0.750}Ni_{0.250}PO_4$

The XRD Analysis shows that 25% atomic ratio of Nickel was successfully doped in $LiFePO_4$. The XRD pattern matched the XRD peaks of $LiFePO_4$ but at the same time few peaks of $LiNiPO_4$ also matched.

FE SEM images showed the presence of grains as well as amorphous (possibly) material. The percentage of grains decreases as the percentage of nickel increases. The average grain size is around 2.15µm for this composition. EDS Analysis of the whole sample shows the presence of elements in the proper ratio.

Sad image Figure: 45 (e) shows the sad pattern of a single crystal. The sad image may have been taken in a single crystal region.

4.4 $LiFe_{0.625}Ni_{0.375}PO_4$

$LiFe_{0.625}Ni_{0.375}PO_4$'s XRD shows clear peaks which matches with the peak of $LiFePO_4$ and also matches with few peaks of $LiNiPO_4$. The EDS Analysis does not match with the atomic percentage composition of $LiFe_{0.625}Ni_{0.375}PO_4$. This may be due to the presence of more amorphous material. Well developed grains could not be seen. As expected the amorphous nature is dominating in this case. The same conclusion can be arrived at with the SAD images.

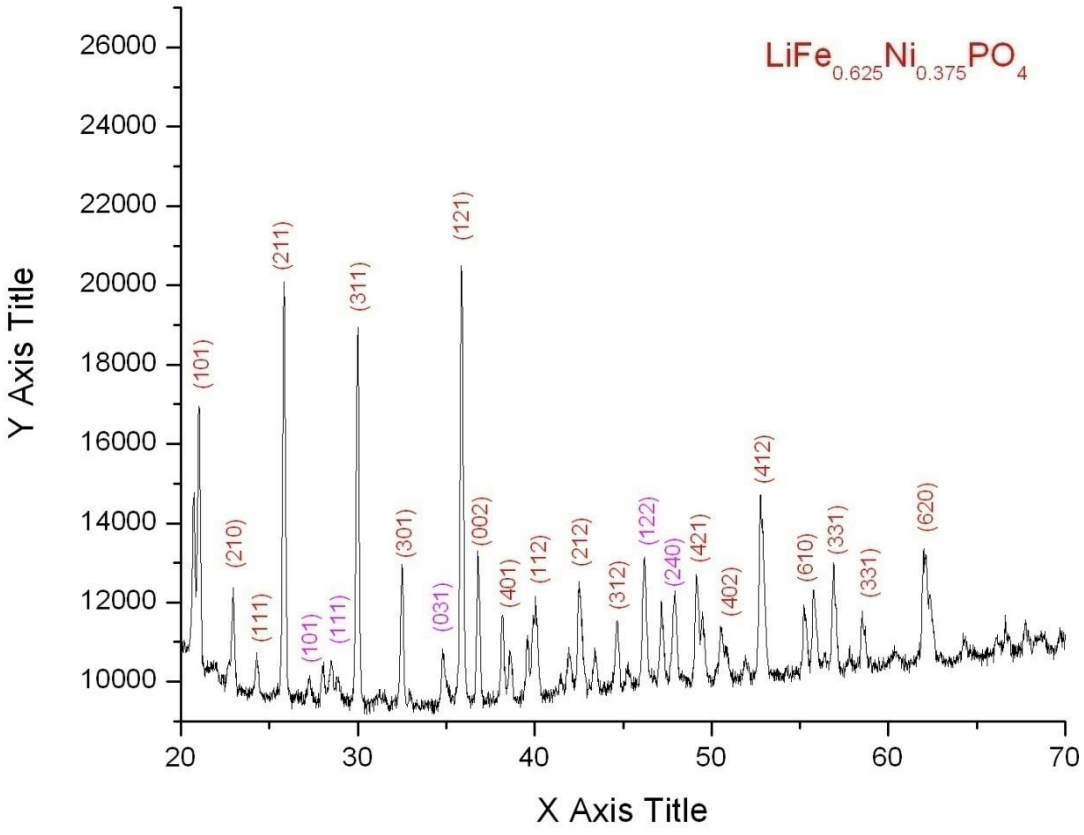

Figure 46: XRD of $LiFe_{0.625}Ni_{0.375}PO_4$

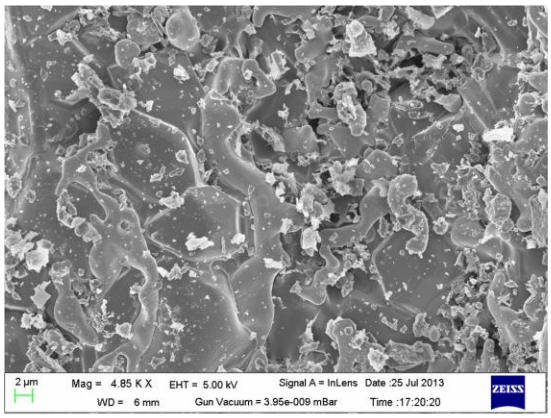

(a)

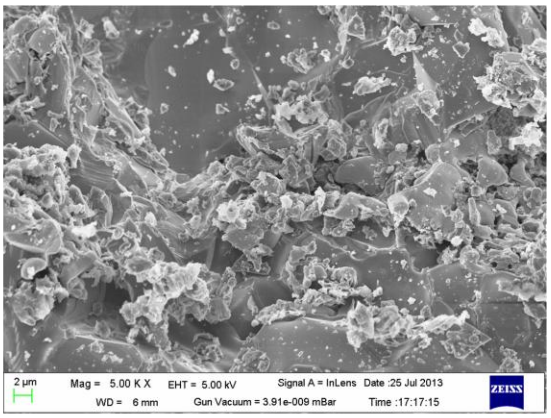

(b)

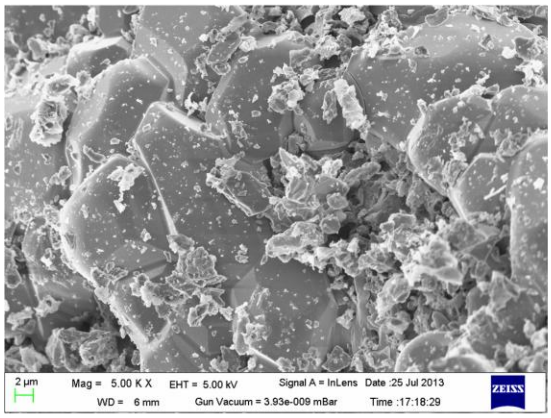

(c)

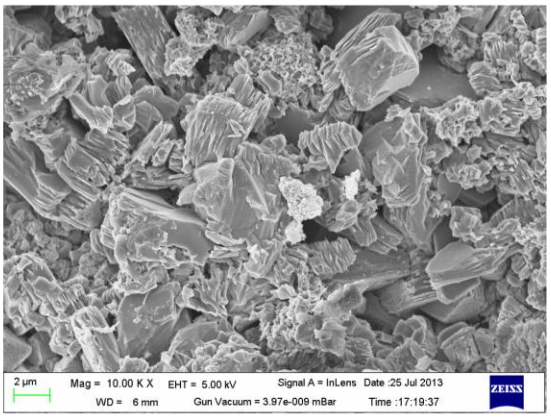

(d)

Figure 47: FESEM Images of $Li_{0.625}Ni_{0.375}PO_4$

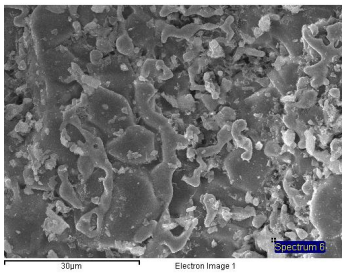

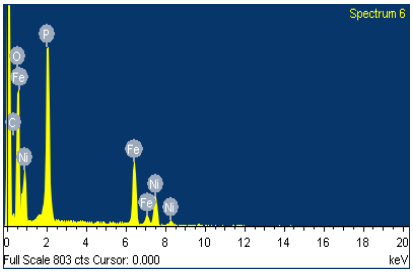

Element	Weight%	Atomic%
C K	9.08	17.37
O K	39.12	56.17
P K	16.50	12.23
Fe K	20.61	8.48
Ni K	14.70	5.75
Totals	100.00	

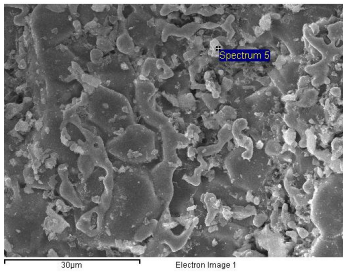

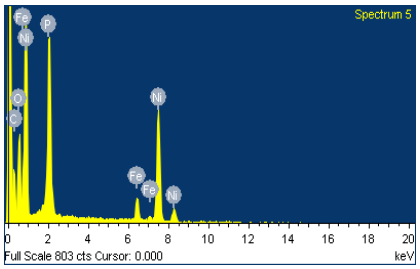

Element	Weight%	Atomic%
C K	30.99	53.00
O K	20.70	26.58
P K	10.99	7.29
Fe K	3.92	1.44
Ni K	33.41	11.69
Totals	100.00	

Figure 48: EDS Analysis of $Li_{0.625}Ni_{0.375}PO_4$

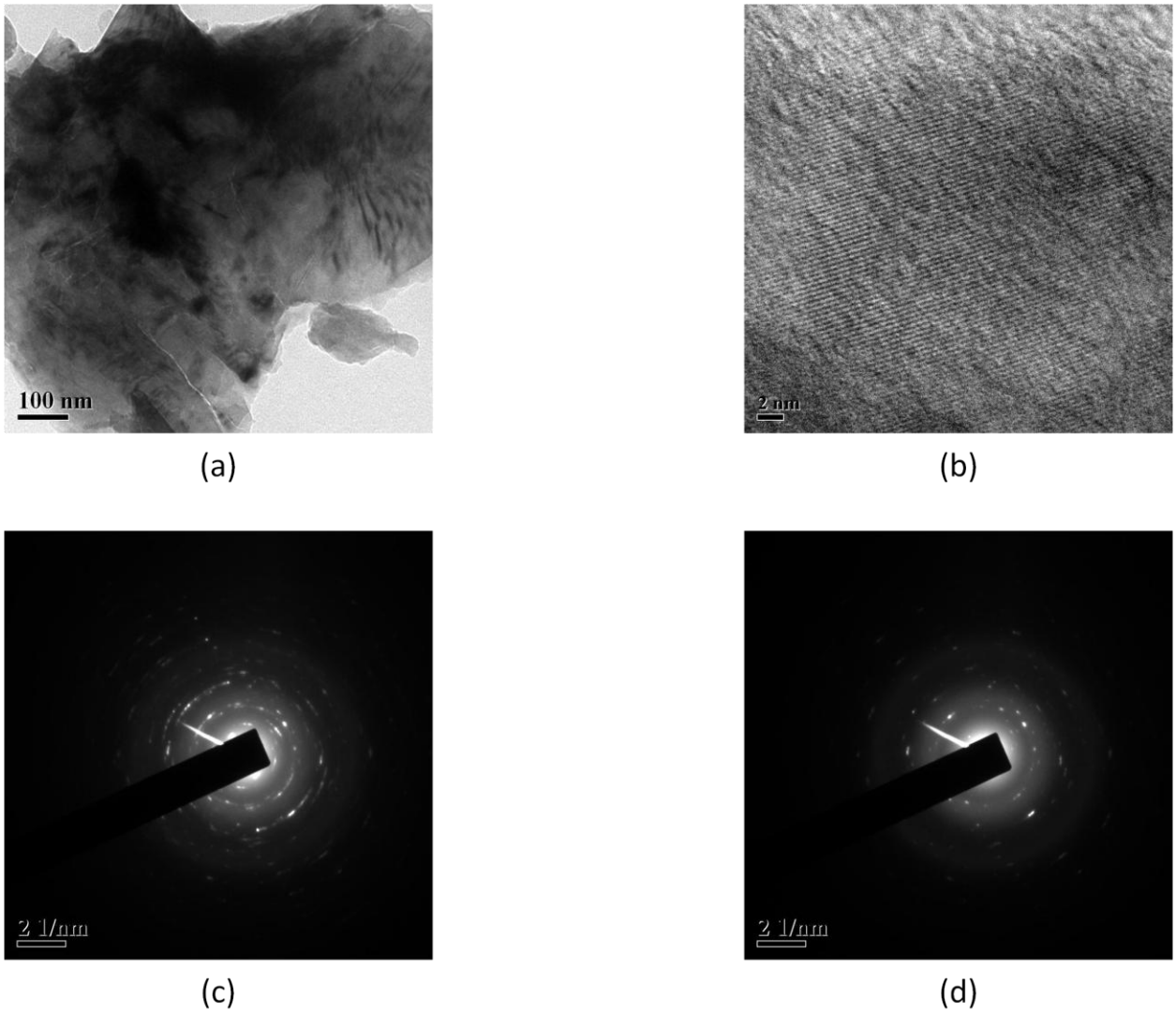

Figure 49: HRTEM Analysis of $Li_{0.625}Ni_{0.375}PO_4$

4.5 $LiNiPO_4$

The XRD Analysis shows that LiNiPO4 peaks were obtained. The $LiNiPO_4$ belongs to the Orthorhombic crystal system, pmnb space group and having 62 space group Number.

The PDF Reference Code NO. 00-032-0578 matches with the $LiNiPO_4$. From the PDF code, the Lattice parameters come out to be:

a=5.8550

b=10.0680

c= 4.6820

α = β = γ = 90°

FE SEM images and sad patterns confirm the presence of amorphous and crystalline material.

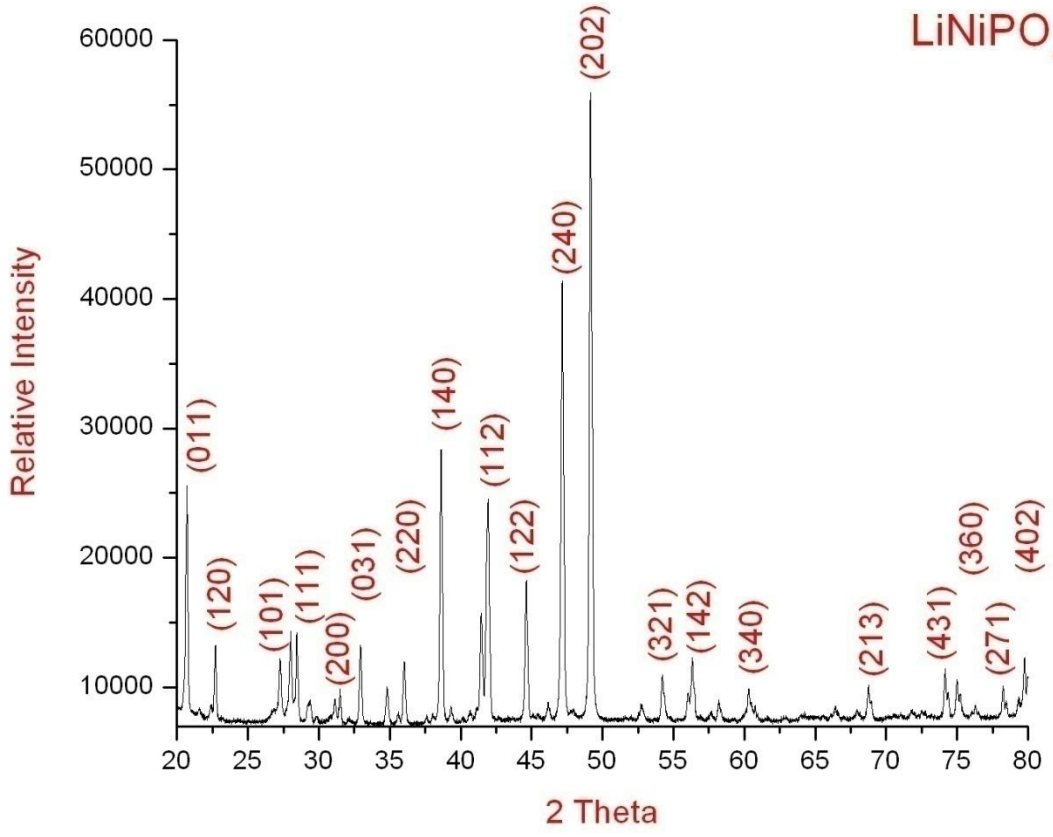

Figure 50: XRD of $LiNiPO_4$

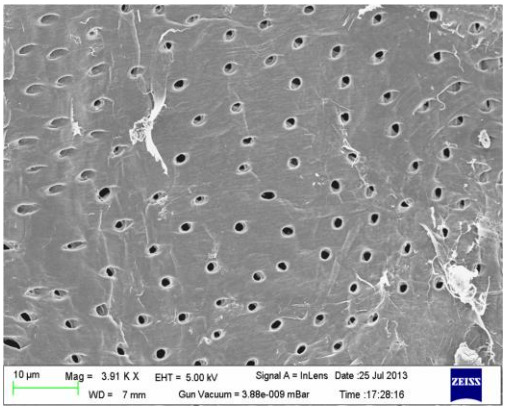

(a)

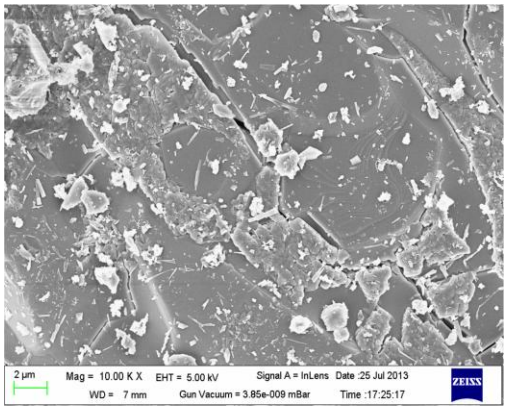

(b)

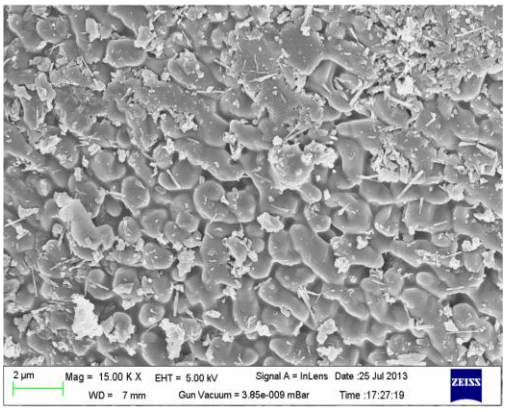

(c)

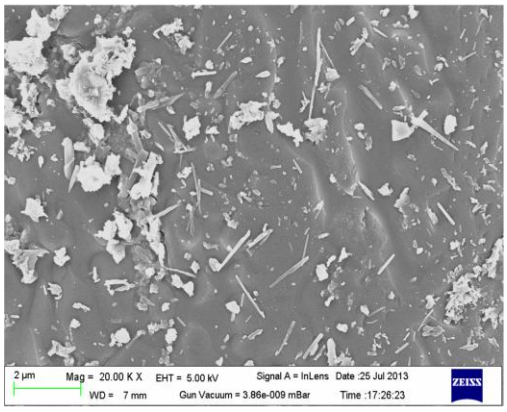

(d)

Figure 51: FE-SEM Pictures of $LiNiPO_4$

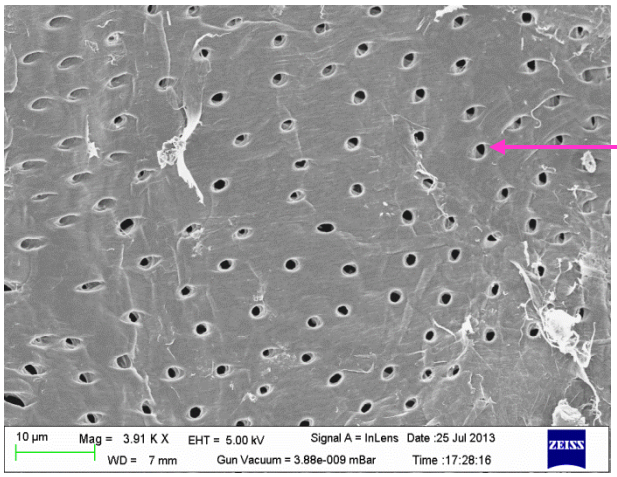

Micro pores

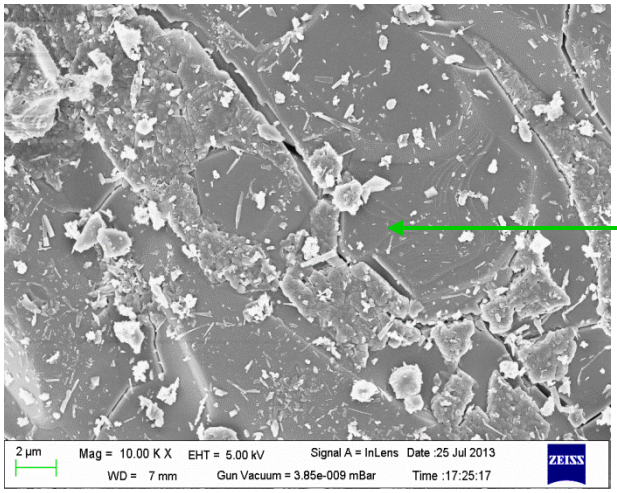

No grain formation at all

Partial grain formation

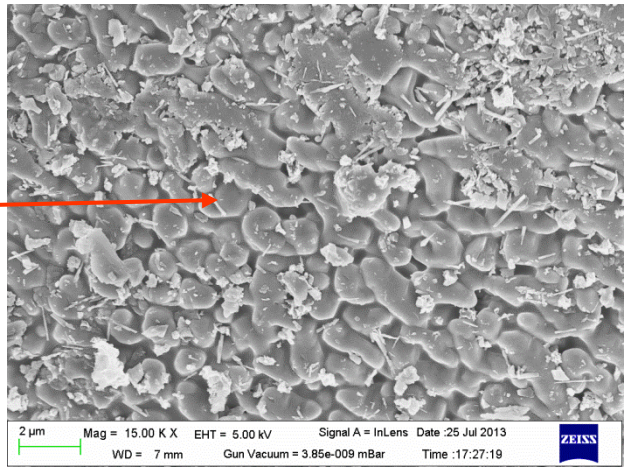

Figure 52: FE SEM Images $LiNiPO_4$

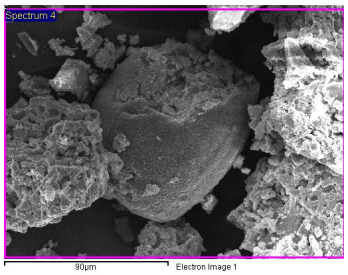

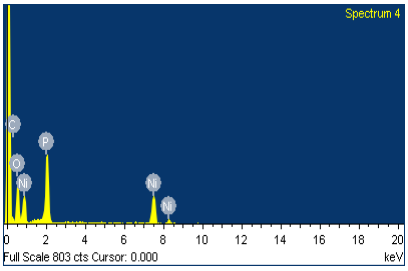

Element	Weight%	Atomic%
C K	15.16	28.37
O K	32.47	45.62
P K	17.36	12.60
Ni K	35.01	13.41
Totals	100.00	

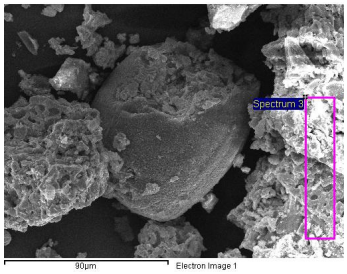

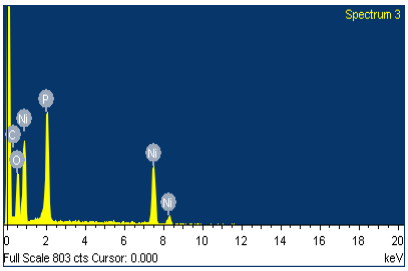

Element	Weight%	Atomic%
C K	0.00	0.00
O K	25.52	49.70
P K	22.68	22.81
Ni K	51.80	27.49
Totals	100.00	

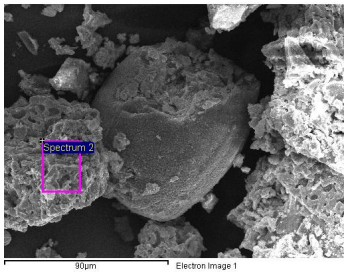

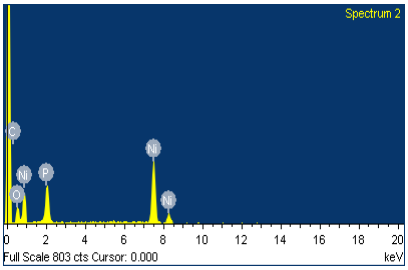

Element	Weight%	Atomic%
C K	0.00	0.00
O K	25.52	49.70
P K	22.68	22.81
Ni K	51.80	27.49
Totals	100.00	

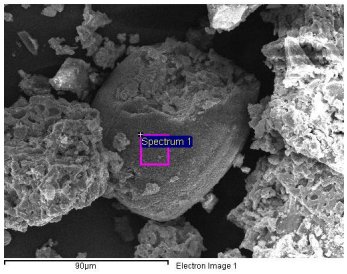

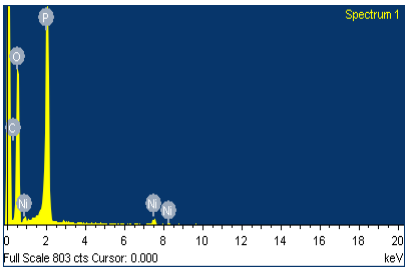

Element	Weight%	Atomic%
C K	0.00	0.00
O K	25.52	49.70
P K	22.68	22.81
Ni K	51.80	27.49
Totals	100.00	

Figure 53: EDS Images of $LiNiPO_4$

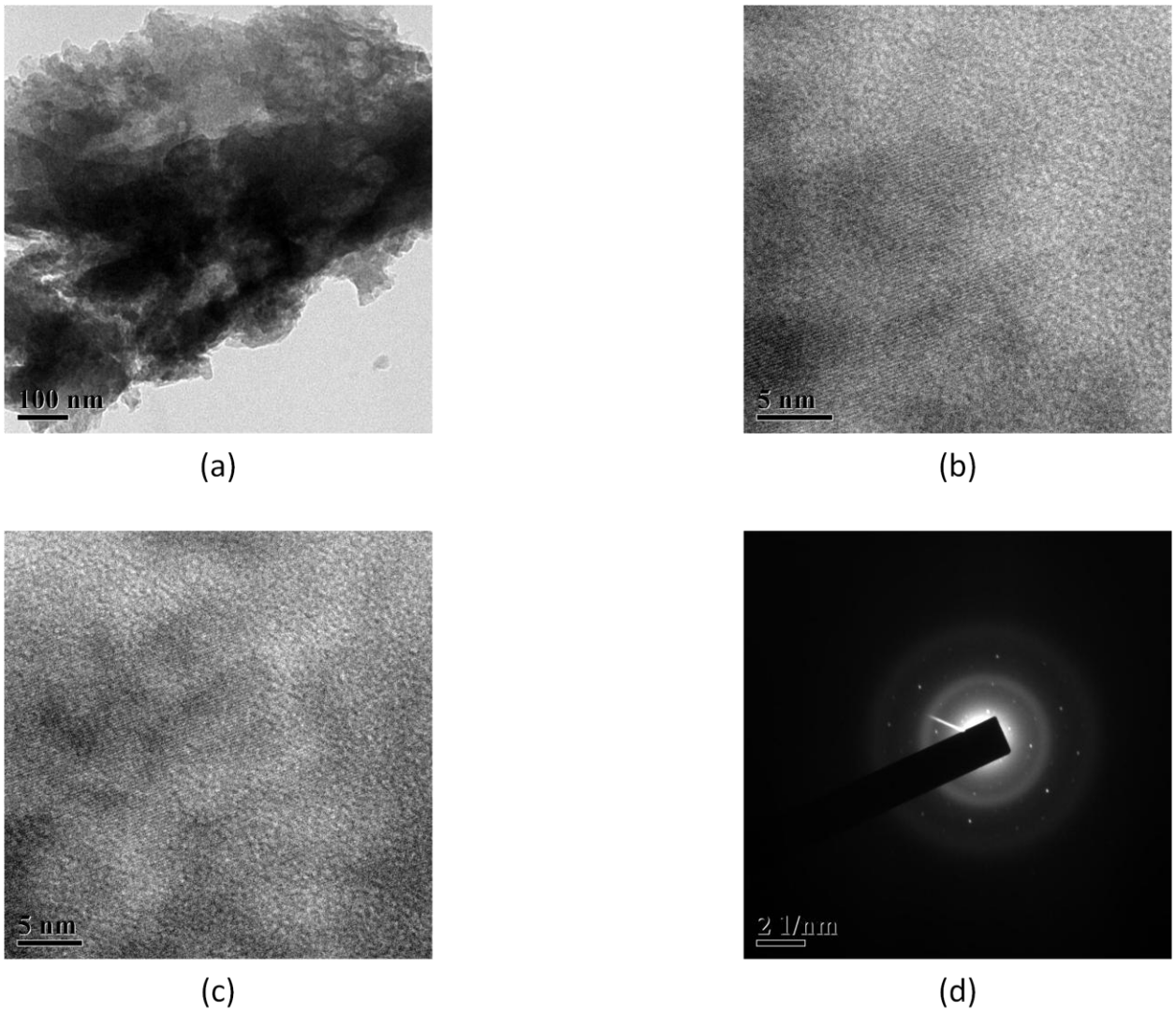

Figure 54: HR-TEM images of $LiNiPO_4$

Chapter 5: Conclusions

- $LiFe_{1-X}Ni_XPO_4$ /C ($0 \leq X \leq 1$) composites have been successfully synthesized by sol gel synthesis route.

- X-Ray Diffraction Analysis shows that $LiFe_{1-X}Ni_XPO_4$ /C ($0 \leq X \leq 1$) shows no diffraction pattern for Carbon which means that carbon is amorphous in nature or insignificant amount of crystalline carbon is present. The structure of the $LiFe_{1-X}Ni_XPO_4$ /C ($0 \leq X \leq 1$) was found to be orthorhombic. The diffraction pattern for $LiFe_{1-X}Ni_XPO_4$ /C ($0 < X < 1$) composites are almost similar to $LiFePO_4$ diffraction pattern except the inclusion of some diffraction peaks of $LiNiPO_4$ for higher value of X. This shows that Nickel doping has been successfully performed.

- With the help of FE-SEM, detail study of surface morphology and chemical composition was done. FE-SEM images have shown that fraction of grain morphology decreases for higher value X. The grain formation in $LiFePO_4$/C is the best whereas in $LiNiPO_4$/C was the worst among all samples. EDS data taken for different samples at different portion of the sample also confirmed this fact.

- With the help of HR-TEM, micrographic images were studied. Selected area diffraction was carried out and Lattice Fringe Images were seen. In a nutshell, the synthesis and characterization of $LiFe_{1-X}Ni_XPO_4$ /C ($0 \leq X \leq 1$) composites has been successfully done.

REFERENCES

1. J. Chen, Recent Progress in Advanced Materials for Lithium Ion Batteries, *Materials* 2013, *6*, 156-183

2. http://en.wikipedia.org/wiki/History_of_the_battery.

3. http://library.thinkquest.org/04apr/00215/applications/personal/timeline%20of%20batteries/battery_timeline.htm.

4. O.Toprakci, H. Toprakci, L. Ji, X. Zhang, Fabrication and Electrochemical Characteristics of LiFePO4 Powders for Lithium–Ion Batteries, Kona Powder and Particle Journal 28(2010) 50-72.

5. A.Patil, V. Patil, D. W. Shin, J. W. Choi, D.S. Paik, S. J. Yoon, Issues and challenges facing rechargeable thin film lithium batteries, Material Research Bulletin 43 (2008) 1913-1942.

6. O.Toprakci, H. Toprakci, L. Ji, X. Zhang, Fabrication and Electrochemical Characteristics of LiFePO4 Powders for Lithium–Ion Batteries, Kona Powder and Particle Journal 28(2010) 50-72.

7. Y. Zhang, Q. Huo, P. Duo, L. Wang, A. Zhang, Advances in new cathode material LiFePO4 for lithium ions batteries, Synthetic Metals 162 (2012) 1315-1326.

8. A. Ritchie, W. Howard, Recent developments and likely advances in Lithium-ion batteries, Journal of Power Sources 162 (2006) 809-812.

9. A.K. Padhi, K.S. Nanjundaswamy , J.B.Goodenough, Phospho-olivines as Positive Electrode Materials for Lithium Batteries, Journal of Electrochemical Society 144 (1997) 1188-1194.

10. G.X. Wang, S. Bewlay, J. Yao, J.H. Ahn, S.X. Dou, Characterization of LiMXFe1-XPO4 (M= Mg, Zr, Ti) cathode materials prepared by the sol-gel method, Electrochemical and Solid-State Letters, 7(2004) A503-A506.

11. S. Yang, Y. Song, P. Y. Zavalij, M. S. Whittingham, Reactivity, Stability and electrochemical behavior of lithium iron phosphates, Electrochemistry Communications 4 (2002) 239-244.

12. R.Dominko, M.Bele, M. Gaberscek, M. Remskar, D. Hanzel, S. Pejovnik, J. Jamnik, Impact of carbon coating thickness on the electrochemical performance of LiFePO4, Journal of the Electrochemical Society 152(2005) A607-A610.

13. J.K. Kim, J. W. Choi, G. S. Chauhan, J.H.Ahn, G.C. Hwang, J.B. Choi, H. J. Ahn, Enhancement of electrochemical performance of lithium iron phosphate by controlled sol gel synthesis, Electrochimica Acta 53(2008) 8258-8264.

14. R. Dominko, M. Bele, M. Gaberscek, M. Remskar, D. Hanzel, S. Pejovnik, J. Jamnik, Impact of the carbon coating thickness on the electrochemical performance of LiFePO4/C Composites, Journal of the Electrochemical Society 152(2005) A607-A610.

15. R. Dominko, M. Bele, M. Gaberscek, M. Remskar, D. Hanzel, J. M. Goupil, S. Pejovnik, J. Jamnik, Porous olivine composites synthesized by sol gel technique, Journal of Power Sources 153(2006) 274-280.

16. http://batteryuniversity.com/learn/article/secondary_batteries

17. D.Lisbona, T.Snee, A review of hazards associated with primary lithium and lithium-ion batteries, Process Safety and Environmental Protection 89 (2011), 434–442.

18. Y. Zhang, Q. Huo, P. Du, L. Wang, A. Zhang, Y. Song, Y. Lv, G. Li, Advances in new cathode material LiFePO4 for lithium-ion batteries, Synthetic Metals 162 (2012), 1315– 1326.

19. T.Ohzuku,R.Brodd, An overview of positive-electrode materials for advanced lithium-ion batteries, Journal of Power Sources 174 (2007) 449–456.

20. A.A Salah, A. Mauger, C.M. Julien, F. Gendron, Nano-sized impurity phases in relation to the mode of preparation of LiFePO4, Materials Science and Engineering B 129 (2006) 232–244.

21. O. Toprakci, H. A.K. Toprakci, L. Ji, X. Zhang, Fabrication and Electrochemical Characteristics Of LiFePO4 Powders for Lithium-Ion Batteries, KONA Powder and Particle Journal No.28 (2010) 50-73.

22. C. M. Hayner, X. Zhao, H. H. Kung, Materials for Rechargeable Lithium-Ion Batteries, Annual Review Chemical &Biomolecular Engineering 3 (2012) 445–471.

23. D. Aurbach, Y. Talyosef, B. Markovsky, E. Markevich, E. Zinigrad, L. Asraf, J. S. 73 Gnanaraj, H.J. Kim, Design of electrolyte solutions for Li and Li-ion batteries: review, Electrochimica Acta 50 (2004) 247–254.

24. S. S. Zhang, A review on electrolyte additives for lithium-ion batteries, Journal of Power Sources 162 (2006) 1379–1394.

25. Y.Ge, X.Yan, J.Liu, X.Zhang, J.Wang, X.He, R.Wang, H.Xie, An optimized Ni doped LiFePO4/C nanocomposite with excellent rate performance, Electrochimica Acta 55(2010) 5886-5890.

26. Y.Ding, P.Zhang, Effect of Mg and Co co-doping on electrochemical-properties of LiFePO4 ,Transactions of Nonferrous Metals Society of China 22(2012) 153-156.

27. H.Liu, Q.Cao, L.J.Fu, C.Li, Y.P.Wu, H.Q.Wu, Doping effects of zinc on LiFePO4 cathode material for Lithium Ion Battery, Electrochemistry Communications8(2006) 1553-1557.

28. C.Li, N.Hua, C.Wang, X.Kang, T.Wuamair, Y.Han, Effect of Mn2+ doping in LiFePO4 and the low temperature electrochemical performances, Journal of Alloys and Compounds 509(2011) 1897-1900.

29. X.Ou, G. Liang, L.Wang, S. Xu, X. Zhao, Effects of magnesiun doping on electronic conductivity and electrochemical properties of LiFePO4 prepared via hydrothermal route, Journal of Power Sources 184(2008) 543-547.

30. C. Delacourt, C. Wurm, L. Laffont, J.-B. Leriche, C. Masquelier, Electrochemical and electrical properties of Nb- and/or C-containing LiFePO4 composites, Solid State Ionics 177 (2006) 333 – 341.

31. C.S. Sun, Z. Zhou, Z.G. Xu, D.G.Wang, J.P.Wei, X.K. Bian, J. Yan, Improved high-rate charge/discharge performances of LiFePO4/C via V-doping, Journal of Power Sources 193 (2009) 841–845.

32. J.Ma,B.Li,F.Kang,ImprovedelectrochemicalperformancesofnanocrystallineLiFePO4/C composite cathode via V-doping and VO2(B) coating, Journal of Physics and Chemistry of Solids 73 (2012) 1463–1468.

33. H. Guo-rong, G. Xu-guang, P. Zhong-dong, D. Ke, T. Xian-yan, L. Yan-jun, Influence of Ti4+ doping on electrochemical properties of LiFeP04/C cathode material for lithium-ion batteries

34. H. Shu, X. Wang, W. Wen, Q. Liang, X. Yang, Q. Wei, B. Hu, L. Liu, X. Liu, Y. Song, M. Zho, Y. Bai, L. Jiang, M. Chen, S. Yang, J. Tan, Y. Liao, H. Jiang, Effective enhancement of electrochemical properties for LiFePO4/C cathode materials by Na and Ti co-doping, Electrochimica Acta 89 (2013) 479– 487.

35. H. C. Shina, S. B. Parka, H. Janga, K. Y. Chungb, W. Chob,C. S. Kimb, B.W. Chob, Rate performance and structural change of Cr-doped LiFePO4/C during cycling, Electrochimica Acta 53 (2008) 7946–7951.

36. H. Liu, Q. Cao, L.J. Fu, C. Li, Y.P. Wu *, H.Q. Wu, Doping effects of zinc on LiFePO4 cathode material for lithium ion batteries, Journal of Alloys and Compounds 477 (2009) 498–503.

37. Q. Zhang, S. Wang, Z. Zhou , G. Ma, W. Jiang, X. Guo, S. Zhao, Structural and electrochemical properties of Nd-doped LiFePO4/C prepared without using inert gas, Solid State Ionics 191 (2011) 40–44.

38. M. Milovi, D. Jugovi, N. C. canin , D. Uskokovi, A. S. M.Sevi, Z. S. Popovi, F. R. Vukajlovi, Crystal structure analysis and first principle investigation of F doping in LiFePO4 Journal of Power Sources 241 (2013) 70-79.

39. J. Xu, C. Jia, B. Cao, W.F. Zhang**,** Electrochemical properties of anatase TiO2 nanotubes as an anode material for lithium-ion batteries, Electrochimica Acta 52 (2007) 8044–80

40. R. Liang, Z. Wang, H. Guo, X. Li, W. Peng, Z. Wang, Fabrication and Electrochemical Properties of lithium-ion batteries for power tools, Journal of Power Sources 184 (2008) 598–603.

41. http://www.isuppli.com/Abstract/P18802_20110804122658.pdf 75